ELSEVIER

Fluid Phase Equilibria, 97 (1994) 211–242

FLUID PHASE EQUILIBRIA

Direct vapor pressure measurements of ten *n*-alkanes in the C_{10}–C_{28} range

David L. Morgan, Riki Kobayashi *

Department of Chemical Engineering, George R. Brown School of Engineering, Rice University, Houston, TX 77251, USA

(Received November 22, 1991; accepted in final form January 1, 1994)

Abstract

Morgan, D.L. and Kobayashi, R., 1994. Direct vapor pressure measurements of ten *n*-alkanes in the C_{10}–C_{28} range. *Fluid Phase Equilibria*, 97: 211–242.

Direct vapor pressure measurements of zone-refined *n*-alkane samples (decane, 323–588 K; dodecane, 352–588 K; tetradecane, 373–588 K; hexadecane, 393–583 K; octadecane, 413–588 K; nonadecane, 423–588 K; eicosane, 433–588 K; docosane, 453–573 K; tetracosane, 453–588 K; and octacosane, 483–588 K) are reported. Most temperature measurements are accurate within ± 0.02 K with a maximum uncertainty estimated at $\Delta T_{exp} = \pm 0.03$ K. The maximum uncertainty of the pressure measurements, which range from 0.082 to 1385 kPa, depends on the measured pressure according to $\Delta P_{exp} = 0.0015P + 0.0048$. The vapor pressures are fitted to a "2.5–5" Wagner equation and shown to be of high precision. The fits are used to make comparisons with selected literature results. Additional fits are presented which combine literature vapor pressures with the new data. These are based on the two-real fluid Corresponding States Principle (CSP) method used by Ambrose and Patel (Ambrose, D, and Patel, N.C., 1984. J. Chem. Thermodyn., 16: 459–468), which has been applied to extrapolate and smooth vapor pressures. Morgan (Morgan, D.L. and Kobayashi, R., 1994. Extension of Pitzer CSP models for vapor pressures and heats of vaporization to long-chain hydrocarbons. *Fluid Phase Equilibria*, 94: 51–87.) has incorporated the experimental measurements into Pitzer-type CSP correlations.

Keywords: Experiments; Data; Method; Vapor–liquid equilibria; *n*-Alkane

1. Introduction

When perturbation methods are applied to a thermodynamic property framework based on *n*-alkanes, properties of other classes of compounds can be estimated. In this paper, we present direct vapor pressure measurements of *n*-alkanes in the C_{10}–C_{28} range which help to fill "gaps"

* Corresponding author.

SSDI 0378-3812(94)02476-H

in the experimental literature and to create a more accurate thermodynamic framework. The results are taken from the Ph.D. thesis of Morgan (1990). Interested readers will find many additional details in that reference. Based on the new measurements and on extensive literature reviews, Morgan (1990) and Morgan and Kobayashi (1991, 1994) have extended the acentric factor range of several Pitzer et al. (1955) three-parameter (T_c, P_c and ω) Corresponding States Principle (CSP) correlations.

Measurements of *n*-alkane vapor pressures from the triple point up to the critical point have been underway for over one hundred years. Because vapor pressures of samples can vary as much as 11 orders of magnitude over the coexistence range, generally no single technique is capable of measuring the entire range. For this reason it is useful to refer to several, somewhat arbitrary, pressure ranges (1 kPa = 7.500 616 8 mm of Hg):

Presure range	mm Hg	kPa
High	10^3–10^5	10^2–10^4
Mid	10^1–10^3	10^0–10^2
Low	10^{-6}–10^1	10^{-7}–10^0

Measurements in the mid-pressure range tend to be of the highest accuracy. High-pressure measurements can be of high accuracy providing that thermal decomposition effects are negligible. Low-pressure measurements are extremely important for characterizing high-molecular-weight hydrocarbons; however, the accuracy of such measurements is easily compromised by the inadequacy of experimental techniques, by various phenomenological effects, and thermal decomposition. For this reason, many efforts have been directed towards the development of low-pressure experimental methods (e.g. Douslin and Osborn, 1965; Carruth and Kobayashi, 1973; Macknick and Prausnitz, 1979; Sasse et al., 1988) and towards the development of correlations for predicting low-pressure vapor pressures from accurate mid-pressure results (e.g. Scott and Osborn, 1979; McGarry, 1983; Ambrose and Patel, 1984; King and Mahmud, 1986).

Although numerous techniques exist for measuring vapor pressures (Partington, 1951; Nesmeyanov, 1963; Hàlla et al, 1967; Weissberger et al., 1971; Ambrose, 1975), only four general methods have been widely applied to the study of organic compounds. These four generic techniques are referred to as the static (direct), ebulliometric (boiling or dynamic), elution (gas saturation, transpiration, transport, flow), and Knudsen effusion methods. We have applied a static method in this work.

Static vapor pressure measurements are also known as "direct" measurements because the equilibrium pressure exerted by a liquid of solid sample, which is maintained at constant temperature, is measured directly by a pressure gauge. Many kinds of pressure gauges have been used including mercury manometers, dead weight piston gauges, Bourdon tubes, and capacitance pressure transducers. Since samples are often corrosive or are taken to temperatures outside the operating range of the pressure gauge, it is usual practice to isolate the sample from the pressure gauge by using a differential pressure indicator (DPI) such as a U-tube manometer filled with mercury or a metal diaphragm. When the DPI indicates that pressures of an inert reference fluid and the sample are equal, the reference fluid pressure is measured using an appropriate pressure gauge.

Direct vapor pressure measurements in the literature have ranged over an astonishingly wide range of pressures (see Ambrose, 1975). Several effects, however, may limit the accuracy of static methods, especially for systems at low pressures or at extreme temperatures. Impurities such as lighter hydrocarbons, decomposition products, dissolved or desorbed gases can easily mask vapor pressures of less volatile hydrocarbons. The liquid and vapor phases of a sample may not be in equilibrium. Equipment, such as temperature and pressure gauges, may not be properly calibrated. If proper precautions are not taken, DPI hysteresis or special transport phenomena such as thermal transpiration, Knudsen flow, and molecular flow (Storvick and Park, 1978; O'Hanlon, 1980) can obscure low-pressure results.

2. Gaps in the literature

Numerous vapor pressure reviews and compilations exist that contain smoothed, correlated, or experimental *n*-alkane data with references (e.g. Krafft, 1882a, b, 1886; Young, 1928; Stull, 1947; Thodos, 1950; Rossini et al., 1953; API, Bibliography, 1964; API-42, 1966; Zwolinski and Wilhoit, 1971; Vargaftik, 1975; Ohe, 1976; McGarry, 1983; Danner and Daubert, 1983; Boublik et al., 1984; Dykyj et al. 1979, 1984; Reid et al., 1987; TRC Thermodynamic Tables on the Hydrocarbons, Texas A & M). Morgan (1990) summarized vapor pressure data ranges and citations for the *n*-alkanes, C_1–C_{43}, in thesis Tables 2.1 and 2.2. Critical and triple point data are referenced elsewhere within the thesis.

To help visualize "gaps" in the *n*-alkane vapor pressure literature, we plotted the ranges of the pressure and temperature measurements versus the carbon number (Morgan, 1990). An initial set of plots was constructed in 1986, before we made our measurements. After we had completed our measurements at the end of 1988, we updated these plots. Figure 1 depicts the early 1989 status. Additional information shown, such as the fixed point loci (triple points, boiling points and critical points), the region where thermal decomposition begins, and regions where special measurement techniques may be required (e.g. direct, elution or effusion), gives insight into the behavior of the normal paraffin series (e.g. triple point CSP) (Morgan and Kobayashi, 1991).

When Fig. 1 was updated by adding the ranges of our measurements and the low-pressure results of Sasse et al. (1988), significant portions of two gaps located below the "onset of thermal decomposition" loci and between C_9 and C_{29} were filled in. The availability of accurate data near $T_r = 0.7$ for C_{18}–C_{28}, significantly improved the quality of our CSP correlations, which depend on accurately determining acentric factors from vapor pressures, (see Eq. (10)). In addition, the new results simplified our task of assessing literature tabulations such as Vargaftik's (1975) and Antoine vapor pressure correlations presented by the Thermodynamics Research Center (TRC) and the API Research Project 44 (Rossini et al., 1953).

3. Experimental

In this section, brief discussions on the materials, apparatuses, temperature and pressure measurements, and procedures are given.

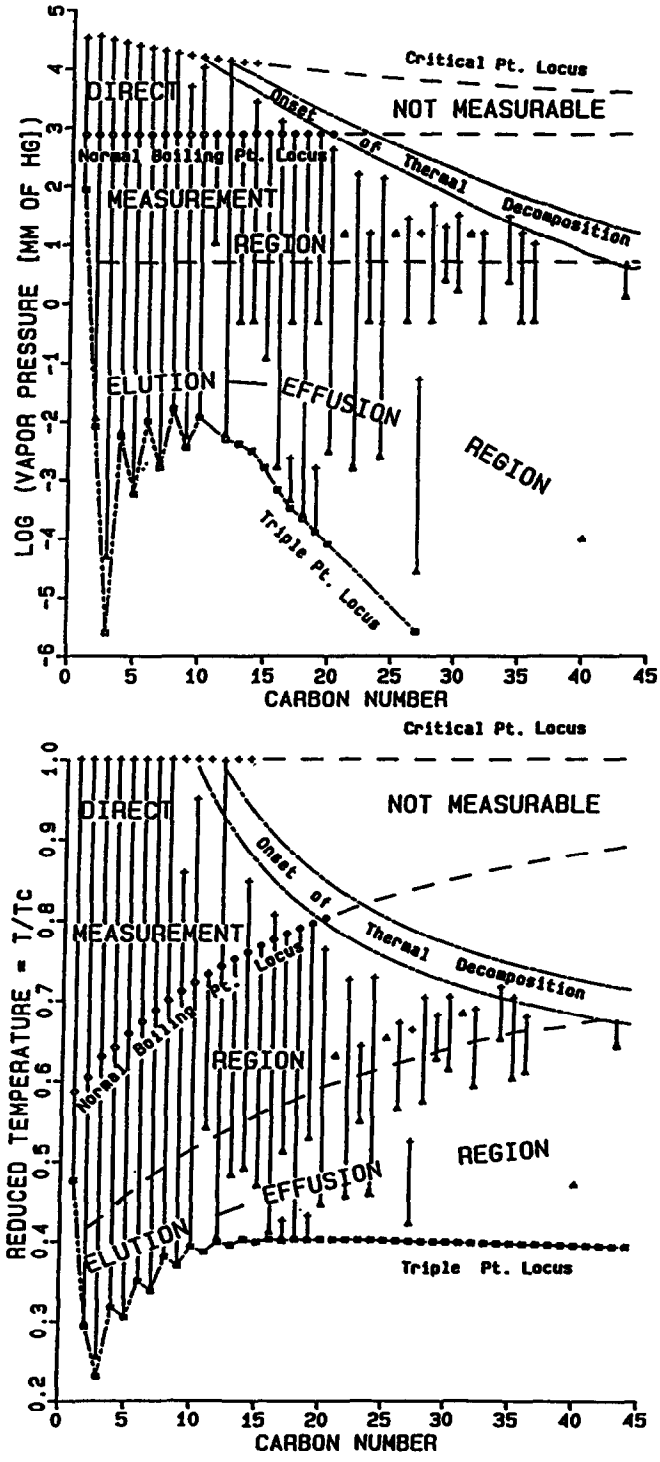

Fig. 1. Composite pressure/temperature ranges of *n*-alkane vapor pressure measurements up to 1989; □, triple point; ○, normal boiling point; ▲, lowest measurement; +, highest measurement.

3.1. Materials

Since use of high-purity samples is crucial for accurately determining vapor pressures, we upgraded the purity of commercial stocks by zone refining (Nasir, 1980; Martin et al. 1984; Morgan. 1990). References by Sloan and McGhie (1988), Wilcox (1964), Herington (1963) and Pfann (1958) discuss the theory of this technique. Table 1 summarizes information about the *n*-alkane samples used in the vapor pressure measurements such as the stock supplier, estimated purity before and after purification, freezing point of a nitrogen-saturated sample, and the boiling point at 10 mm of Hg.

The purities and freezing points reported in Table 1 are the result of applying a freezing curve technique based on Taylor and Rossini (1944) and Glasgow et al. (1945). Each zone-refined ingot was sectioned into four or five cuts which ranged from the top of the column, where traveling liquid zones originated, to the bottom. By testing all cuts, the purest sample could be determined. Freezing point determinations were reproducible, in good agreement with literature results (Morgan, 1990) and other signs of purity such as crystallinity and boiling character-

Table 1
Specification of *n*-alkane samples

Carbon number, *n*	Stock supplier (lot #)	Stock purity (mol%)	Number of zone passes	Est. purity [b] after zone refining (cut)	Sample freez. pt., T_f(K)	10 mmHg boiling pt. [d], T(K)
10	Phillips (1231)	99.85 [a]	0			330.72
12	Aldrich (0109DK)	99.00	36	99.94 (top)	263.696 [c]	364.51
14	Aldrich (3821BL)	99.00	55	99.95 (mid)	279.006	394.73
16	Aldrich (1723PK)	99.00	44	99.94 (mid)	291.302	421.87
18	Alfa (032785)	99.00	44	99.8 ± 0.1 (top)	301.313	446.54
19	Alfa (110885)	99.00	44	99.2 ± 0.1 (top)	304.990	458.08
20	Aldrich (3116KK)	99.00	56 56	99.9 ± 0.1 (top) 99.7 ± (mid)	309.637 309.618	469.67 469.66
22	Aldrich (5117KJ)	99.00	100	99.3 ± 0.5 (top)	317.028	490.58
24	Alfa (070885)	>97.00	48	99.5 ± 0.5 (top)	323.610	510.08
28	Alfa (051685)	99.00	96	99.3 ± 0.6 (mid)	334.208	544.69

[a] Research grade sample analyzed by GLC at Phillips Petroleum Company.
[b] Estimated by a freezing curve method based on Glasgow et al. (1945).
[c] The thermopile used in this measurement was not calibrated below 273 K.
[d] Calculated from vapor pressure fits given in Table 4 (10 mmHg = 1.33322 kPa).

istics. For example, freezing curve studies indicated that separation of impurities along the zone-refined C_{19} ingot was poor. All of the C_{19} cuts lacked the crystalline appearance of the other studied paraffins and felt sticky when touched. When degassing the C_{19} sample prior to making vapor pressure measurements, an excessive amount of volatile impurities had to be boiled off into the vacuum system.

3.2. Vapor pressure apparatus

The static vapor pressure apparatus used in this study is depicted in Fig. 2 and is similar in design to apparatus used in previous works (Nasir, 1980; Nasir et al., 1980; Wieczorek and Kobayashi, 1980; Sivaraman and Kobayashi, 1982; Sivaraman et al. 1983; Roper, 1988). A thermostat (constant temperature bath) is raised hydraulically up to the major components of the apparatus which hang downward from an insulated platform called the bulkhead. When the thermostat is lowered, the equipment is accessible for servicing.

Major components of the static vapor pressure apparatus are identified in Fig. 2. These include the equilibrium cell (EC), a container designed to allow vapor from a sample to attain equilibrium with its liquid; the magnetic slusher (MS), which facilitates the approach of the sample to equilibrium; a null-type differential pressure indicator (DPI), which isolates pressure-measuring devices (DWG, DDR, Heise Gauge and TV) from the sample and indicates when the pressure of a nitrogen reference gas equals the sample vapor pressure; a hand-operated proportioning pump that enables fine balancing of the reference nitrogen pressure; a hydraulically driven propeller for stirring the bath; a nitrogen purge system for blanketing the bath fluid

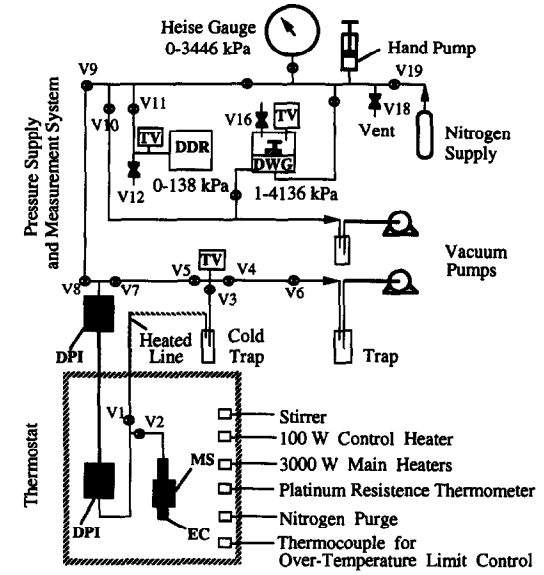

MS = Magnetic Slusher
EC = Equilibrium Cell
DWG = Air Dead Weight Gauge
DDR = Digital Quartz Pressure Gauge
DPI = Differential Pressure Indicator
TV = Thermovac Vacuum Gauge

Fig. 2. Static vapor pressure apparatus.

under nitrogen and testing the integrity of the thermostat bath flange/bulkhead seal; a platinum resistance thermometer for bath temperature control and measurement; a thermocouple for bath temperature overshoot control, a 100 W immersion heater for fine temperature control; a combination of strip heaters which provide up to 3000 W for coarse temperature control of the thermostat.

Modifications made to the apparatus since the work of Sivaraman et al. (1983) include: replacement of the magnetic pump for circulating vapor through the liquid equilibrium cell (Ruska et al., 1970) with a magnetic slusher (Roper, 1988); use of a paraffinic oil bath fluid (Multitherm Corporation IG-2) instead of a eutectic mixture of inorganic salts; implementation of a computerized temperature controller and measurement readout system; use of an auxiliary system to bake out the equilibrium cell and charge it with sample; general upgrades to the vacuum manifold which eliminated unnecessary valves, bends, tubing, etc.

3.3. Bath temperature control and measurement readout

A base heat load for temperature control or for rapidly increasing the temperature of the thermostat was provided by manually adjusting the output of the 3000 W main heater. Fine temperature control over a 10 K range was attained by use of the 100 W immersion heater which provided an output according to a proportional-offset control loop and a programmable power supply. The control algorithm was incorporated into a BASIC program which ran on a Commodore microcomputer. The computer addressed peripherals such as the the controller power supply and a Keithley Model 192 Programmable digital multimeter (DMM) over an IEEE-488 interface. When the control algorithm required the temperature of the bath, the computer instructed the Keithley DMM to make a four-wire resistance measurement of a 500 Ω Omega platinum resistance thermometer (PRT) which was mounted in the thermostat bath. The resulting measurement was conveyed to the computer, converted to a temperture, then displayed on the computer's display. In a similar manner, the voltage output of a Ruska DDR-6000 pressure transducer was converted to a pressure reading by the computer and displayed.

During a typical 1–2 h vapor pressure measurement period, the thermostat was controlled within ± 0.004 K. For periods in excess of 8 h, control could be maintained within a standard deviation of ± 0.01 K.

3.4. Temperature measurements

Temperature measurements were made using the same 500 Ω Omega PRT/Keithley DMM system used to control the bath temperature; however, final reported temperatures for vapor pressure measurements are based on the painstaking comparison of the 500 Ω Omega PRT (model PR-11-3-500-1/4-17.5-E) with two different Leeds & Northrup 25 Ω precision PRTs with calibration traceable to NBS. (Note: NBS is now called NIST, the US National Institute of Standards and Technology). The resistances of the precision thermometers were measured by Leeds & Northrup Mueller bridges which were independently calibrated against a standard resistor traceable to NBS. The Omega PRT/Keithley DMM measurement system was shown to be self-consistent over the duration of the vapor pressure experiments. The final calibration curves were etablished by following temperature paths similar to those followed during vapor pressure measurements.

All temperature measurements are expressed according to IPTS-68 (Comité International des Poids et Mesures, 1969; Benedict, 1984). Most are expected to be accurate within ±0.02 K with a maximum error estimated to be 0.03 K. Thus a recommended value for the uncertaintly in temperature measurements, ΔT_{exp}, is

$$\Delta T_{exp} = 0.03 \text{ K} \tag{1}$$

We have reported our temperatures in terms of IPTS-68 to maintain consistency with our correlation work (Morgan, 1990; Morgan and Kobayashi, 1994). To convert them to the International Temperature Scale of 1990 (ITS-90), one can use the Table 1 corrections given in the NIST Technical Note 1265 (Mangum and Furukawa, 1990). We fit the difference between the two temperature scales, $\delta(t) = t_{90} - t_{68}$, as a function of the Celsius temperature, $t = T - 273.15$, between −190 and 600°C, to an eighth order polynomial:

$$\delta(t) = -2.3248\text{e-}04t - 7.0424\text{e-}07t^2 + 4.0232\text{e-}09t^3 + 1.0349\text{e-}11t^4 - 3.8395\text{e-}14t^5 - 7.4309\text{e-}17t^6 + 2.8635\text{e-}19t^7 - 2.0818\text{e-}22t^8 \tag{2}$$

The standard deviation of the fit, which used 80 points, is 0.00050°C. The maximum deviation, 0.00118°C, occurs at −180°C. Equation (2) should never be applied outside of its fit range.

Although most applications do not require the temperature scale to be adjusted, Eq. (2) can be applied in precise work to rectify the temperature scale of the experimental and correlation results of this work. Adding $\delta(t)$ to our temperature measurements will convert them to ITS-90. The magnitude of the corrections ranges from 0.0°C at 0.0°C to −0.040°C at 250.0°C. To adjust the temperature scale of correlations and data fits, ITS-90 temperatures must be converted back to IPTS-68 by subtracting $\delta(t)$ from ITS-90 temperatures at which calculations are made.

3.5. Pressure measurements

The vapor pressure measurements of this work depended on the use of a null-type differential pressure indicator (DPI) which allowed the direct comparison of sample vapor pressure with nitrogen reference gas pressure. The position of a metal diaphragm in the DPI which separated the sample from the reference gas was first measured when an equal reference pressure was applied to both sides of the diaphragm. Then, with the sample exerting its pressure on one side of the diaphragm and the reference gas on the othe side, the reference pressure was adjusted until the initial null positon of the diaphragm was reproduced. After the null state of the DPI was re-established, an assortment of pressure gauges were used to measure the pressure of the reference gas.

3.5.1. Differential pressure indicator (DPI)

The DPI used was manufactured by the Ruska Instrument Corporation and consisted of a model 2439-702-046 differential pressure null transducer (DPNT) and a model 2416-708-00 differential pressure null indicator (DPNI). The lower cylinder of the dumbbell-shaped DPNT was mounted in the thermostat bath at the same level as the equilibrium cell. It contained the thin metallic diaphragm which separates the reference gas in the upper chamber from the sample vapors below. A slim metal rod attached to the top of the diaphragm extended out of the bath

through a 52 cm long hollow shaft to the upper cylinder of the DPNT. This portion of the DPNT contained a transformer which sensed the position of the diaphragm. Multiple wire leads from the DPNT fed the information to the DPNI, a box which contained electronics, a null indicator meter and a couple of potentiometers for adjusting the gain and the position of the null meter needle. The meter was delineated by divisions in units of two ranging from −50 to +50 meter units (MU).

The DPI sensitivity, which is defined as the ratio of the change in reference gas pressure to the resulting change in meter reading, $\Delta P/\Delta MU$, was determined by slightly over- or under-pressurizing the reference gas to produce a shift in the DPNI readout of about 10 MU away from the zero position. Usually the sensitivity ranged between 0.001 3 and 0.001 7 kPa MU^{-1}. Knowledge of the sensitivity of the DPI enabled the calculation of "null shift" corrections which were added to pressure measurements under 7.33 kPa. Null shifts occurred for some of the measurements because the steady-state temperature distribution within the thermostat's insulation lagged behind the bath fluid's steady-state temperature after changing the bath's temperature. Changes in insulation temperature during the course of a vapor pressure measurement sometimes affected the length of the DPI connecting rod. By accounting for small shifts in the null meter readout after completing vapor pressure measurements, the precision of low-pressure measurements could be significantly enhanced.

To minimize mechanical stresses on the DPI diaphragm which might adversely affect low-pressure measurements, the reference pressure used to determine the null position of the DPI was adjusted to the same pressure magnitude as the vapor pressure to be measured. For example, a pressure of 1.33 kPa might be used to measure a 0.67 kPa vapor pressure, but not a 101 kPa pressure because it would be too dissimilar.

3.5.2. Pressure and vacuum gauges

Several pressure and vacuum gauges are indicated in the pressure supply and measurement system of the vapor pressure apparatus schematic (Fig. 2). All reported pressure measurements, however, are ultimately related to a model 2465 Ruska Instrument Corporation air dead weight gauge (DWG) with calibration traceable to NBS and to "zero pressures" determined by Leybold-Heraeus model TM 220S2 Thermovac vacuum (TV) gauges.

The DWG was used in two modes. For absolute pressures between 1.38 and 138 kPa (0.2–20 psia), it served to calibrate a Ruska model DDR-6000-151-20 digital pressure gauge (DDR), a highly precise and linear pressure transducer which uses a fused quartz Bourdon tube. For pressures above 138 kPa, the DWG was used to measure the pressure of the nitrogen reference gas.

There is little difference between the two DWG operation modes. In the calibration mode, the bell jar which encloses the piston and cylinder assembly of the DWG was evacuated to a reference pressure of 0.0133 kPa as determined by a TV mounted on top of the bell jar. In a high-pressure measurement mode, the atmospheric pressure was used as a reference pressure. Air was admitted into the DWG bell jar and into the DDR through a Drierite-packed drying tube. In this way, the DDR served as an accurate barometer to measure the bell jar pressure.

All final DWG pressure measurements were corrected to allow for the influence of temperature on the DWG piston's effective area, the buoyancy force of the reference gas on the weights and piston inside the bell jar, and the effects of the local acceleration due to gravity.

For measuring nitrogen reference gas pressure less than 138 kPa, the DDR was used. The DC voltage output of the DDR varied linearly from 0 to 10 V (0 to 138 kPa) and could be accurately measured using the Keithley DMM. To ensure its reproducibility, however, the DDR had to be referenced to a "zero pressure" prior to each pressure measurement. This was achieved by evacuating the DDR and a TV mounted beside it to a pressure between 0.011 and 0.013 kPa, and then adjusting a DDR potentiometer until the DDR pressure readout agreed with the TV readout.

For pressures above 138 kPa where the DDR could not be used, a Heise model H46360 Bourbon tube gauge rated for the 0–3446 kPa range allowed quick pressure measurements needed to leak-test the pressure supply system and to null the DPI.

3.5.3. Expected accuracy of pressure measurements

The overall uncertainty in pressure measurements, ΔP_{exp}, was postulated to depend proportionally on the pressure of the reference gas and on a hypothetical zero pressure uncertainty, ΔP_0:

$$\Delta P_{exp} = kP + \Delta P_0 \tag{3}$$

In accord with calibration results for the DWG which the Ruska Instrument Corporation provided, k was assumed to be 0.000 15. ΔP_0 was estimated by applying a gaussian error propagation formula to components of the zero-pressure uncertainty:

$$\Delta P_0 = \left|(\Delta P_{DDR})^2 + 2(\Delta P_{TV})^2 + (\Delta P_{DPI})^2\right|^{1/2} \tag{4}$$

Components of the zero-pressure uncertainty include the error in the DDR pressure gauge reading, ΔP_{DDR}, the errors of the two Thermovac vacuum gauges used in the calibration/measurement procedures, ΔP_{TV}, and the uncertainty introduced when finding the null position of the DPI, ΔP_{DPI}.

Since the Keithley DMM voltage measurement error could be safely neglected, the uncertainty in the DDR pressure gauge measurements, $\Delta P_{DDR} = 0.0025$ kPa, was estimated as twice the standard deviation of a linear fit which compared the differences between the readings of the DWG and DDR pressure gauges versus the uncorrected DDR pressure readings.

The Thermovac vacuum gauges affiliated with the DDR and DWG operation had a stated uncertainty of ± 1 linear scale division, which in the 0.011–0.013 kPa pressure range translates to ± 0.0020 kPa. Assuming this value, $\Delta P_{TV} = 0.0020$ kPa.

The uncertainty in the DPI null was assumed to be two DPNI meter units, i.e. twice the DPI sensitivity, $\Delta P_{DPI} = 0.002\,93$ kPa. This value is reasonable for pressures below 7.33 kPa since stress/strain effects on the DPI diaphragm are very small. At the highest pressures encountered in this work, the proportional term dominates Eq. (3).

Thus, according to Eqs. (3) and (4) and the zero-pressure uncertainties, when the pressure, P, is measured in kPa, its expected uncertainty in kPa is

$$\Delta P_{exp} = 0.00015P + 0.0048 \tag{5}$$

3.6. Procedures

The vapor pressure apparatus and the equilibrium cell (EC) were cleaned separately before a sample was introduced. First, the EC was removed from the apparatus and replaced by a

cleanup plug. The cold trap in Fig. 2 was removed from the apparatus, cleaned, then re-attached. Finally, the thermostat was ramped to its maximum operating temperature, 588 K, and held at that temperature for 2–12 h while the apparatus baked out under vacuum.

The EC was cleaned with solvents after disassembly, reassembled, then attached to an auxiliary apparatus which was used to bake out the sample container at high temperatures and to charge it with a sample. Typically, the EC was baked for at least 24 h at 623 K while under a high vacuum, then cooled to a temperature above the melting point of the sample to be studied. Approximately 33 cm^3 of liquid sample was charged into the EC, which had a total capacity of 53 cm^3. Finally, the EC was re-attached to the cleaned vapor pressure apparatus.

Before vapor pressure measurements commenced, samples were purged of volatile impurities and air residues. A two-stage "degassing" procedure was followed. In the first stage, a series of freeze–evacuation–thaw cycles were followed. To determine if a sample had melted and to facilitate liquid mixing, a piston inside the EC, which was made of a magnetic alloy, could be moved up and down by coupling it to the motion of an external magnetic collar (i.e. the magnetic slusher). The freeze–evacuation–thaw cycles were repeated until no difference in pressure could be detected by a Thermovac vacuum gauge which monitored the process.

The second stage, a distillation procedure, commenced with the initial vapor pressure measurement. The thermostat bath temperature was ramped up to a set point where the sample vapor pressure was less than 1.33 kPa. After the temperature of the bath stabilized to within ± 0.004 K of the set point, the null position of the DPI was determined by subjecting both sides of the DPI diaphragm to the same nitrogen reference pressure and finding the DPNI setting which zeroed the meter readout. The nitrogen gas on the sample side of the DPI was then thoroughly evacuated while maintaining nitrogen on the reference side. To distill off volatiles, the vapor space at the top of the equilibrium cell was opened directly to the vacuum as the magnetic slusher mixed the sample. Periodically, the EC and DPI were isolated from the vacuum so that a non-equilibrium sample pressure could be determined. After numerous repetitions, the sample pressure approached a minimum value and the sample was essentially degassed.

Initial vapor pressure measurements at low pressures were unreliable, because any liquid sample that pooled against the DPI diaphragm as a result of the distillation procedure would require a long time to evaporate. To address this problem, a second vapor pressure measurement was made at a higher temperture at which the DPI would rapidly dry out. If the sample vapor pressure was below 6.7 kPa, the procedures of the first measurement were followed; otherwise, more care was taken during the degassing step not to withdraw a large portion of the sample into the vacuum system.

After a sample was degassed, the evacuated sample side of the DPI was isolated from the vacuum manifold and the sample in the EC was opened to the DPI and allowed to approach equilibrium for several minutes. With the magnetic slusher turned off, the reference gas pressure was adjusted to null the DPI readout. DDR pressure measurements were recorded every minute for up to 20 min while manually balancing the reference pressure to maintain the DPI readout meter in a zero position. The sensitivity of the DPI was determined. After isolating the EC from the DPI, residue sample vapors were evacuated from the sample side of the DPI and the null state of the DPI was verified. Null shift corrections which were applied to some of the vapor pressure measurements below 7.33 kPa are reported in Table 5.3 of Morgan (1990).

Once the high-temperature measurement was completed, the sample was considered degassed for lower-temperature measurements. The bath temperature was lowered in an incremental manner. Only small amounts of sample vapor were bled into the vacuum to expel residue nitrogen gas from the sample side of the DPI. The high-temperature degassing of samples enabled the measurement of vapor pressures as low as 0.13 kPa without flooding the DPI.

After vapor pressure measurements at the lower temperatures were obtained, the bath temperature was ramped upwards in increments to study the range above 500 K. Excess bath fluid was siphoned off to account for thermal expansion. Since most of the paraffins exhibit thermal decomposition, the measurements were made quickly to minimize the build-up of volatile decomposition products. Attempts were made to degas samples thoroughly. For vapor pressures above 138 kPa, the upper pressure limit for the DDR, the air dead weight pressure gauge was used to measure the reference pressure.

4. Results

Tables 2 and 3 summarize our resulting vapor pressure measurements. Extra decimal places are included to maintain the internal consistency of the data. The number of significant digits can be estimated by applying Eqs. (1) and (5). For precise work, temperatures can be converted from IPTS-68 to ITS-90 by application of Eq. (2).

In the remaining subsections of this section, we present fits of the data using a Wagner vapor pressure equation form, give a brief error analysis of the vapor pressure measurements, and make comparisons with selected literature results.

4.1. Direct fits of vapor pressures

In accordance with Ambrose (1986), we have fitted the vapor pressures of this work to a "2.5–5" form of the Wagner vapor pressure equation:

$$\ln P_r = \frac{C_1 x + C_2 x^{1.5} + C_3 x^{2.5} + C_4 x^5}{T_r} \tag{6}$$

where $T_r = T/T_c$ is the reduced temperature, $P_r = P^S/P_c$ is the reduced vapor pressure, T_c and P_c are the critical temperature and pressure reducing parameters, and the independent variable $x = 1 - T_r$ is a measure of the distance from the critical point.

Desirable features of Wagner equations include accurate interpolation between mid-pressure range data and the critical point, and accurate extrapolation of mid-pressure range data towards low reduced temperatures. McGarry (1983) applied a "3–6" Wagner equation form in his constrained fitting method of limited range data. Ambrose and Patel (1984) used a Wagner equation to represent real reference fluids in the Generalized Corresponding States Principle (GCSP) of Teja (1980) and Teja et al. (1981). We have applied the Ambrose and Patel method extensively in our studies of long-chain *n*-alkanes, Morgan (1990, 1994). Some results are given in Subsection 4.3.4. of this article on "conformal" fits.

Table 4 presents Wagner equation coefficients for the *n*-alkane vapor pressures given in Tables 2 and 3. In each case, data were made dimensionless by use of the T_c and P_c correlations of Twu

Table 2
Experimental vapor pressures of the *n*-alkanes C_{10}–C_{18}

T(K)	P(kPa)	T(K)	P(kPa)	T(K)	P(kPa)
n-Decane					
323.079	0.8741	413.122	38.892	533.129	598.79 [b]
333.083	1.509	433.123	69.685	553.130	830.15 [b]
353.088	4.050	453.124	117.25	573.130	1125.9 [b]
373.120	9.562	473.126	187.25 [b]	588.132	1395.0 [b]
393.121	20.150	493.126	285.77 [b]		
393.121	20.154	513.127	420.38 [b]		
n-Dodecane					
353.119	0.7338	453.124	39.125	553.130	375.27 [b]
373.120	2.031	473.125	67.572	573.131	528.82 [b]
393.071	4.912	493.126	110.50	588.132	671.13 [b]
413.077	10.690	513.126	172.41 [b]		
433.123	21.248	533.129	258.71 [b]		
n-Tetradecane					
373.076	0.4429	493.126	44.274	553.130	177.57 [b]
393.086	1.227	503.114	57.442	573.130	261.56 [b]
413.096	3.026	513.127	73.530	583.132	314.05 [a,b]
433.106	6.693	523.129	93.059	588.132	343.45 [a,b]
453.115	13.526	533.129	116.50		
473.126	25.267	533.129	116.52 [b]		
n-Hexadecane					
393.046	0.3176 [a]	463.093	6.921	533.129	54.642
403.053	0.5412	473.126	9.774	543.129	69.438
413.059	0.8861	483.106	13.530	553.130	87.294
423.066	1.408	493.126	18.414	563.130	108.62
433.072	2.172	503.119	24.691	573.130	133.94
443.079	3.273	513.127	32.600	583.132	163.53 [b]
453.085	4.810	523.129	42.464		
n-Octadecane					
413.069	0.2656	473.126	3.870	528.129	22.730
423.074	0.4436	483.126	5.566	543.129	34.026
433.080	0.7294	493.126	7.834	558.130	49.559
443.086	1.148	503.127	10.835	573.130	70.49
453.124	1.761	513.127	14.744	588.132	98.24 [a]
463.098	2.637	528.129	22.736		

[a] Weighted zero in Wagner equation fit because value exhibited low precision or the effects of decomposition.
[b] Pressure measured using an air dead weight gauge.

(1984). A MINPACKD subroutine called LMDIF1 was used to perform the data regression. Since a weighting factor of 0 or 1 was applied directly to the residual, $(\ln P_{r_{calc}} - \ln P_{r_{exp}})_i$, of each vapor pressure point (see the footnotes to Tables 2 and 3), these fits are referred to as "direct" fits by Morgan and Kobayashi (1994). Weighting factors of 0 eliminated contributions of graphically inconsistent points.

Table 3
Experimental vapor pressures of the *n*-alkanes C_{19}–C_{28}

T(K)	P(kPa)	T(K)	P(kPa)	T(K)	P(kPa)
n-Nonadecane					
423.044	0.2550	483.089	3.570	543.129	24.055
433.052	0.4354	493.096	5.116	558.130	35.684
443.059	0.6914	503.104	7.211	573.130	51.76
453.067	1.076	513.111	9.974	588.132	73.66 [a]
463.074	1.636	523.120	13.555		
473.082	2.444	533.129	18.232		
n-Eicosane (top-cut of zone-refined ingot)					
433.053	0.2440	483.126	2.301	543.129	17.040
443.06	0.4018	493.097	3.358	558.130	25.738
453.068	0.6411	503.104	4.812	573.130	37.745
463.076	1.006	513.111	6.771	588.132	54.21 [a]
473.084	1.537	523.119	9.359		
473.126	1.538	533.129	12.738		
n-Eicosane (mid-cut of zone-refined ingot)					
432.997	0.2449	493.044	3.349	553.107	22.549
443.003	0.4010	503.061	4.813	563.117	29.252
453.010	0.6390	513.065	6.773	573.120	37.754
463.025	0.9991	523.081	9.349	583.132	48.08
473.024	1.541	533.088	12.736		
483.034	2.302	543.099	17.029		
n-Docosane					
453.068	0.2432	493.097	1.480	533.120	6.330
463.076	0.3942	503.127	2.186	543.129	8.695
473.083	0.6287	513.112	3.181	558.130	13.648
483.090	0.9767	523.120	4.524	573.130	20.720
n-Tetracosane					
453.066	0.0901	503.100	1.001	558.130	7.303
463.075	0.1547	513.110	1.506	573.130	11.47
473.082	0.2570	523.121	2.209	588.132	17.46
483.089	0.4156	533.129	3.176		
493.096	0.6529	543.129	4.489		
n-Octacosane					
483.090	0.0821	518.116	0.4453	563.130	2.626
493.097	0.1368	523.120	0.5533	573.130	3.704
503.104	0.2226	533.129	0.8506 [a]	583.132	5.140
508.108	0.2813	543.129	1.255	588.132	6.001
513.111	0.3560	553.130	1.834		

[a] Weighted zero in Wagner equation fit because value exhibited low precision or the effects of decomposition.

Table 4
Direct fits [a] of *n*-alkane vapor pressure data in Tables 2 and 3

Carbon number, *n*	Critical parameters [b]		Acentric factor [c], ω	Wagner equation coefficients [a]				Fit std. dev. [d] (%)
	T_c (K)	P_c (kPa)		c_1	c_2	c_3	c_4	
10	618.86	2119.6	0.4823	−8.4291	2.0672	−3.8215	−4.8457	0.14
12	659.48	1823.2	0.5642	−8.6543	1.7061	−3.8448	−6.4870	0.05
14	693.55	1590.0	0.6455	−8.8670	1.3454	−3.9625	−7.3495	0.28
16	722.59	1404.3	0.7219	−9.3718	1.9330	−5.3984	−6.3172	0.20
18	747.68	1252.8	0.7994	−8.7686	−0.9202	−1.7413	−13.4163	0.24
19	759.01	1187.5	0.8370	−11.1306	6.1148	−13.1631	9.2117	0.40
20 (top) [e]	769.63	1128.0	0.8751	−12.6519	9.7909	−17.4365	9.8701	0.29
20 (mid) [e]	769.63	1128.0	0.8746	−12.9478	10.7221	−18.8496	12.4374	0.37
22	789.02	1023.8	0.9491	−11.9874	6.8481	−13.7083	2.1228	0.22
24	806.31	935.7	1.0236	−11.2450	3.5501	−9.1470	−8.5039	0.10
28	835.88	795.9	1.1634	−18.5113	23.2953	−37.3663	33.1479	0.39

[a] Wagner vapor pressure equation, Eq. (6).
[b] T_c and P_c are defined by correlations of Twu (1984).
[c] Used fitted vapor pressure in Pitzer et al. (1955) definition, Eq. (10).
[d] The percentage deviation of the fit is defined by Eq. (7).
[e] "top" and "mid" refer to a top- and a mid-cut of a zone-refined C_{20} ingot.

The percentage standard deviation given in Table 4 for each fit is defined by the following equation:

$$\sigma \equiv 100\sqrt{\sum_{i=1}^{N} N[(P^s_{calc} - P^s_{exp})_i/(P^s_{exp})_i]^2/(N-M)} \tag{7}$$

whre P^s_{calc} and P^s_{exp} are the calculated and experimental pressures of the ith vapor pressure point, N is the total number of vapor pressure points, $M = 4$ is the number of Wagner vapor pressure equation coefficients, and $N > M$. The fits for C_{10}, C_{12}, and C_{24} are the most precise. These all have standard deviations of less than 0.15%. The least precise fits are those for C_{19}, C_{20}^{mid}, and C_{28}, which average around 0.39%. The relatively low precision of the C_{19} data was probably the result of an impurity which zone refining failed to remove from the sample. Decomposition at the higher temperatures also adversely affected the measurements. We attribute the lower precision of the C_{20} mid-cut data to operator inexperience since this was the first sample to be studied. Finally, the poor results for the C_{28} fit reflect the nature of low-pressure measurements and our application of the vapor pressure apparatus at its low-pressure limits.

In Figs. 3–5, we depict a series of deviation plots for the fits of Table 4. Percentage pressure deviations, $100(P^s_{calc} - P^s_{exp})/P^s_{exp}$, which compare the calculated and experimental vapor pressures, are plotted versus temperature for each sample studied. The effects of decomposition can be seen in the deviation plots for C_{14}, C_{18}, C_{19} and C_{20} as the temperature approaches its

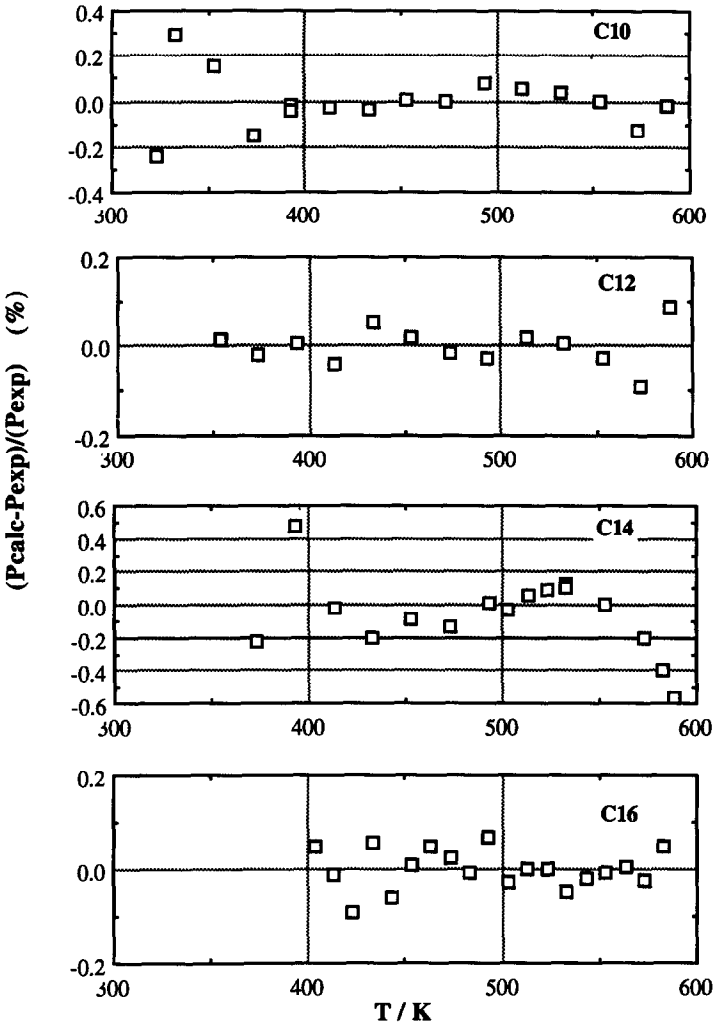

Fig. 3. *n*-Alkane vapor pressures in Table 2 compared with direct fits in Table 4.

maximum value of about 588 K. As Fig. 4 shows, measurements of the top-cut of C_{20} below 583 K are more precise than the lower-temperature results obtained for the mid-cut of C_{20}. Again, we attribute the difference to operator experience. In Fig. 5, we used the fit of top-cut C_{20} data to predict the mid-cut measurements. The deviation plot is similar to the mid-cut deviation plot of Fig. 4 except that it is displaced by a -0.12% bias. The 0.3 mol% difference in cut purity had little influence on the C_{20} vapor pressure measurements.

4.2. Error analysis

The overall accuracy of the direct vapor pressure measurements depends on the accuracy of the individual temperature and pressure measurements as well as on the influence of impurities

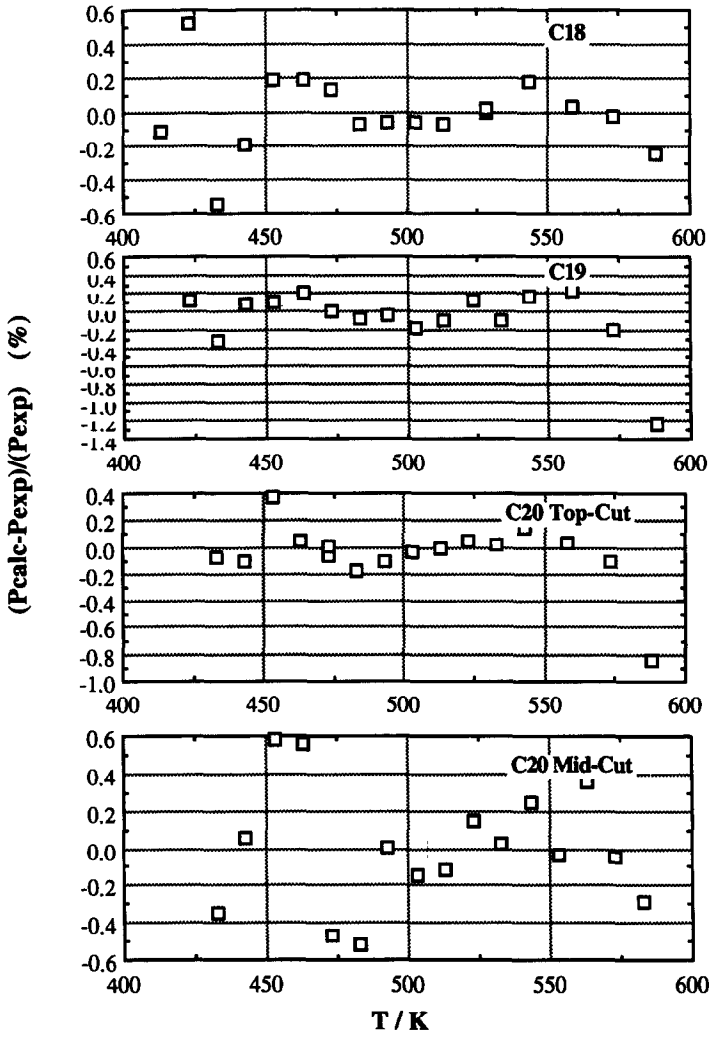

Fig. 4. *n*-Alkane vapor pressures in Tables 2 and 3 compared with direct fits in Table 4.

and other factors such as thermal transpiration (Storvick and Park, 1978). If the effects of impurities and other sources of errors are ignored, then each vapor pressure determination can be represented as a function of temperature and pressure measurements, ie. $P^s = P^s(T, P)$. An overall expected error in the vapor pressure determination, ΔP^S_{tot}, can be calculated by combining estimated errors in the temperature and pressure measurements, ΔT_{exp} and ΔP_{exp}, in an error propagation formula (Olofsson et al. 1981). A gaussian error propagation formula which is widely used for vapor pressures is

$$\Delta P^s_{tot} = \left| \left(\frac{\partial P^s}{\partial T} \right)^2 (\Delta T_{exp})^2 + (\Delta P_{exp})^2 \right|^{1/2} \tag{8}$$

where $\partial P^s/\partial T$ is the slope of the vapor pressure curve estimated from the Wagner equation fits in Table 4, and where ΔT_{exp} and ΔP_{exp} are estimated by Eqs. (1) and (5), respectively.

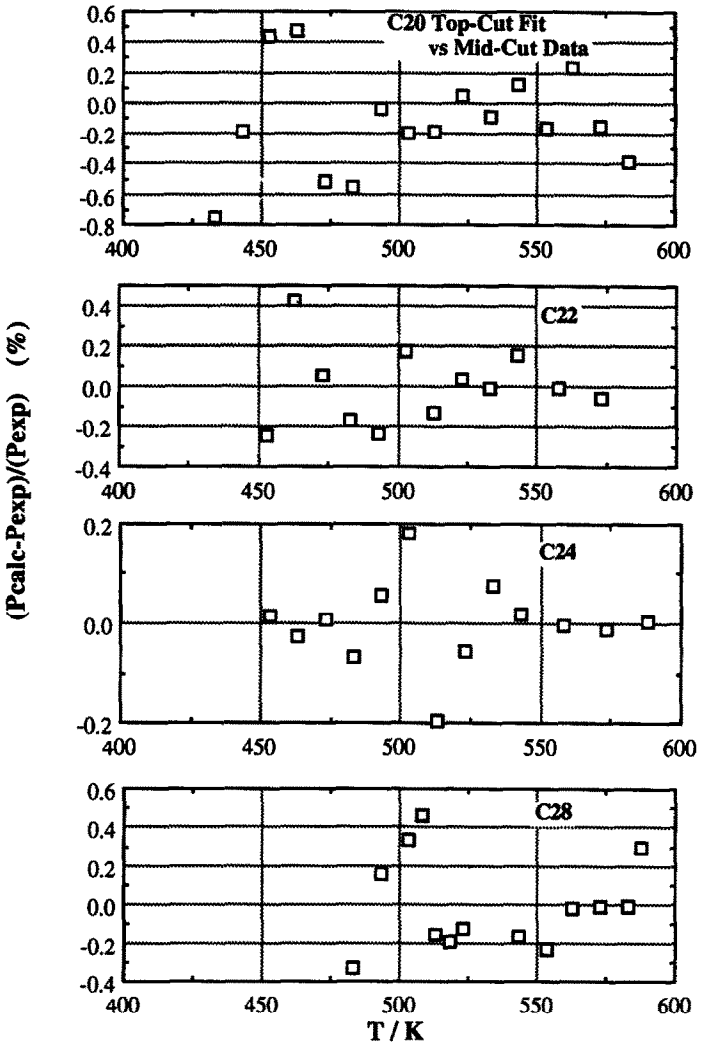

Fig. 5. *n*-Alkane vapor pressures in Table 3 compared with direct fits in Table 4.

Studies of binary mixtures show that impurities can significantly influence the accuracy of thermodynamic property measurements (Eubank et al., 1987; Gallagher and Morrison, 1987). We do not attempt to model impurity effects quantitatively on the vapor pressure measurements because the exact nature of the impurities is unknown. Most probably the impurities consist of paraffinic homologs with molecular weights similar to that of the main component. Crude overall estimates of sample purities are given in Table 1.

The presence of air in an incompletely degassed sample, or of hydrogen and lighter alkenes from thermal cracking of paraffin samples, can have a profound effect on the direct vapor pressure measurements. Cracking was evident at temperatures above 513 K as a slow increase in sample pressure. While most of the lighter breakdown products could be removed by periodically bleeding small portions of the sample into the vacuum system, this approach was less

effective for paraffins having higher vapor pressure ($<C_{20}$). For example, we observed an initial pressure reading of 163.53 kPa when studying hexadecane at 583 K. After 5 h, the pressure increased to 165.04 kPa. Repeated attempts to bleed off lighter impurities proved futile. On this basis, we assigned zero weights to some of the vapor pressure points in Table 2 when fitting the data.

4.3. Literature comparisons

To compare our measurements with literature results, we present a table of vapor pressure citations and a series of deviation plots.

The bibliography for *n*-alkane vapor pressures is given in Table 5. Temperature and pressure ranges, estimated sample purity, and experimental methods (direct, gas saturation, boiling or effusion) are indicated with each citation. The listed purity of some samples is based on conjecture. For example, Allemand et al. (1986) indicated the supplier of their compounds, but not the purity of their samples. We assumed that only the purest Fluka grades were used. Similarly, we assumed that the purity of API-42 samples is similar to the purity of stocks which are available through an API Standard Reference Materials catalog.

In Figs. 6–9, we present a series of deviation plots which use the direct vapor pressure fits of Table 4 to compare our *n*-alkane data with selected literature results. Data from Vargaftik (1975) for C_{18}, C_{19} and C_{20} are included in the plots. Vargaftik cites Tatevskiy (1960); however, we were unable to ascertain the experimental or correlational nature of these data. TRC has issued Antoine vapor pressure correlations which are applicable for specific pressure ranges. These ranges have been adhered to in the deviation plots. The low-pressure TRC correlations for C_{10}–C_{20} are taken from Table 23-2-(1.01)-ka, dated 30 June, 1974. Mid-pressure TRC results for C_{12} to C_{20} are from Table 23-2-(1.01)-k, dated 31 October, 1970. The mid- and high-pressure correlations for C_{10} were obtained from Table 23-2-(1.01)-kb, dated 30 June, 1974. Finally, the TRC correlations for C_{22} to C_{28} are from Table 23-2-(1.02)-k, which was dated 31 October, 1972 and corrected on 30 June, 1984.

4.3.1. Mid-pressure range

The highest quality mid-pressure data in the literature are from systematic studies conducted by APIRP-44 (Willingham et al., 1945; Camin et al., 1954; Camin and Rossini, 1955) for C_{10}–C_{16} and by NIPER, the US National Institute for Petroleum and Energy Research (Douslin and Osborn, 1965; Chirico et al., 1989) for C_{10}, C_{20} and C_{28}. Meyer and Stec (1971) present some ebulliometric measurements of a zone-refined C_{24} sample. In general, our results are in excellent agreement with these sources. The largest discrepancies are the 3% deviations in the C_{28} plot, Fig. 9, which may be ascribed to experimental difficulties encountered by Chirico et al. at the higher temperatures, or possibly by the effects of impurities on our mesurements. Our C_{24} results are about 1% higher than the results of Meyer and Stec.

Older mid-pressure data from Krafft (1882a) for C_{10}–C_{19} are systematically higher than results of modern studies such as APIRP-44 or this work. Data from Myers and Fenske (1955) for C_{16}, C_{18} and C_{20} show appreciable scatter when compared with our results. Agreement with TRC's Antoine fits in the C_{18}–C_{20} range is poor. TRC's C_{19} correlation is based on Krafft's data whereas their fits for C_{18} and C_{20} used results from Myers and Fenske. Except at temperatures near 600 K where our direct fits are as much as 2.5% higher, agreement with Vargaftik's (1975) data for C_{18}, C_{19} and C_{20} is excellent.

Table 5
Vapor pressure bibliography for *n*-alkanes studied

References	Data ranges				Mol% (sample note)	Method [a]
	Temp. (K)		$Log_{10}(P/kPa)$			
C_{10}						
Morgan (1990)	323	588	−0.06	3.15	99.85 (Phillips)	1
Chirico et al. (1989)	268	490	−1.77	2.43	99.998	1, 3
Allemand et al. (1986)	298	348	−0.74	0.50	>99.5 (Fluka Pruiss. *)	2
Carruth and Kobayashi (1973)	243	310	−2.76	−0.69	99.85	2
Willingham et al. (1945)	367	448	0.88	2.02	>99.6	3
Reamer et al. (1942)	311	511	−0.30	2.65		3
Linder (1931)	271	283	−1.24	−0.83		3
Krafft (1882a)	330	446	0.17	2.00		3
C_{12}						
Morgan (1990)	353	588	−0.13	2.83	99.94 (top-cut)	1
Sasse et al. (1988)	264	371	−3.23	0.27	>98. (Fluka purim.)	1
Allemand et al. (1986)	298	390	−1.76	0.63	99.5 (Fluka puriss. *)	2
API-42 (1966)	377	420	0.43	1.12	99.97 (API-ref *)	3
Keistler et al. (1952)	363	486	0.12	2.00		3
Willingham et al. (1945)	399	490	0.80	2.02	>99.94	3
Beale and Docksey (1935)	300	658	−1.71	3.25		1, 3
Krafft (1882a)	364	488	0.17	2.00		3
C_{14}						
Morgan (1990)	373	588	−0.35	2.54	99.95 (mid-cut)	1
Allemand et al. (1986)	343	395	−1.14	0.12	>99.5 (Fluka puriss. *)	2
API-42 (1966)	342	394	−1.18	0.12	99.93 (API ref. *)	3
Ward et al. (1954)	435	518	0.82	1.93	>98.7	3
Camin and Rossini (1955)	428	527	0.74	2.01	99.93 ± 0.06	3
Krafft (1882a)	396	526	0.17	2.00		3
C_{16}						
Morgan (1990)	393	583	−0.50	2.21	99.94 (mid-cut)	1
Eggersten et al. (1969)	299	413	−3.68	−0.09		2
API-42 (1966)	367	421	−1.18	0.12	99.96 (API ref. *)	3
Myers and Fenske (1955)	354	559	−1.57	2.00		3
Camin et al. (1954)	463	560	0.84	2.00	99.96 ± 0.04	3
Bradley and Shellard (1949) fit	293	308	−3.90	−3.21		4
Parks and Moore (1949) fit	298	323	−3.72	−2.63		4
Francis and Wood (1926)	411	437	−0.15	0.41		3
Krafft (1882a)	424	561	0.17	2.00		3
C_{18}						
Morgan (1990)	413	588	−0.58	1.99	99.8 (top-cut)	1
Allemand et al. (1986)	335	440	−2.94	0.00	99. (Fluka puriss. *)	2
Macknick and Prausnitz (1979)	318	361	−3.66	−2.01	>99.	2
API-42 (1966)	389	447	−1.18	0.12	99.90 (API ref. *)	3
Myers and Fenske (1955)	375	568	−1.57	1.82		3
Krafft and Shellard (1882a)	448	590	0.17	2.00		3
Bradley and Shellard (1949) fit	303	313	−4.44	−3.94		4

Table 5

References	Data ranges				Mol% (sample note)	Method [a]
	Temp. (K)		$Log_{10}(P/kPa)$			
C_{19}						
Morgan (1990)	423	588	−0.59	1.87	99.2 (top-cut)	1
API-42 (1966)	402	459	−1.18	0.12		3
Morecroft (1964)	306	328	−4.73	−3.68		4
Krafft (1881a)	459	603	0.17	2.00		3
C_{20}						
Morgan (1990)	433	588	−0.61	1.73	99.9 (top-cut)	1
Morgan (1990)	433	583	−0.61	1.68	99.7 (mid-cut)	1
Chirico et al.(1989)	388	626	−1.81	2.08	99.95	1, 3
Sasse et al. (1988)	363	467	−2.63	0.10	>98. (Fluka purum.)	1
Macknick and Prausnitz (1979)	344	380	−3.39	−2.04	>99.	2
Shiessler and Whitmore (1955)	410	470	−1.18	0.12	(API-42)	3
Myers and Fenske (1955)	395	573	−1.57	1.60		3
Krafft (1882b)	481	481	0.30	0.30		3
C_{22}						
Morgan (1990)	453	573	−0.61	1.32	>99. (top-cut)	1
Sasse et al. (1988)	353	462	−3.70	−0.40	>95. (Fluka purum.)	1
Francis and Wood (1926)	475	513	−0.18	0.52	(synth. hydrocarbon)	3
Krafft (1882b)	504	504	0.30	0.30		3
C_{24}						
Morgan (1990)	453	588	−1.07	1.24	>99. (top-cut)	1
Sasse et al. (1988)	373	462	−3.59	−0.83	>97. (Fluka pract.)	1
Meyer and Stec (1971)	499	565	−0.08	0.95	(100 zone passes)	3
API-42 (1966)	447	511	−1.18	0.12		3
Mazee (1948)	472	494	−0.58	−0.06		3
Francis and Wood (1926)	472	537	−0.70	0.57	(C & CO fractions)	3
Krafft (1882b)	524	524	0.30	0.30		3
C_{28}						
Morgan (1990)	483	588	−1.09	0.78	>99. (mid-cut)	1
Chirico et al. (1989)	453	575	−1.88	0.59	99.984	1, 3
API-42 (1966)	480	545	−1.18	0.12		3
Mazee (1948)	494	522	−0.82	−0.28		3
Francis and Wood (1926)	514	572	−0.53	0.57	(F & FO fractions)	3

[a] 1, direct or static; 2, gas saturation; 3, dynamic or boiling point; 4, effusion.

* Purities not stated. Listed most pure Fluka samples for Allemand et al. (1986) and purities given in API Standard Reference Materials catalog for API-42.

4.3.2. High-pressure range

If we exclude measurements of critical points such as those by Rosenthal and Teja (1989) for C_5–C_{18}, only three literature studies present vapor pressures in the high-pressure region. The C_{10} data of Reamer et al. (1942), which are not depicted in Fig. 6, show poor agreement with this work. In contrast, the high-pressure results of Chirico et al. (1989) for C_{10} are in excellent

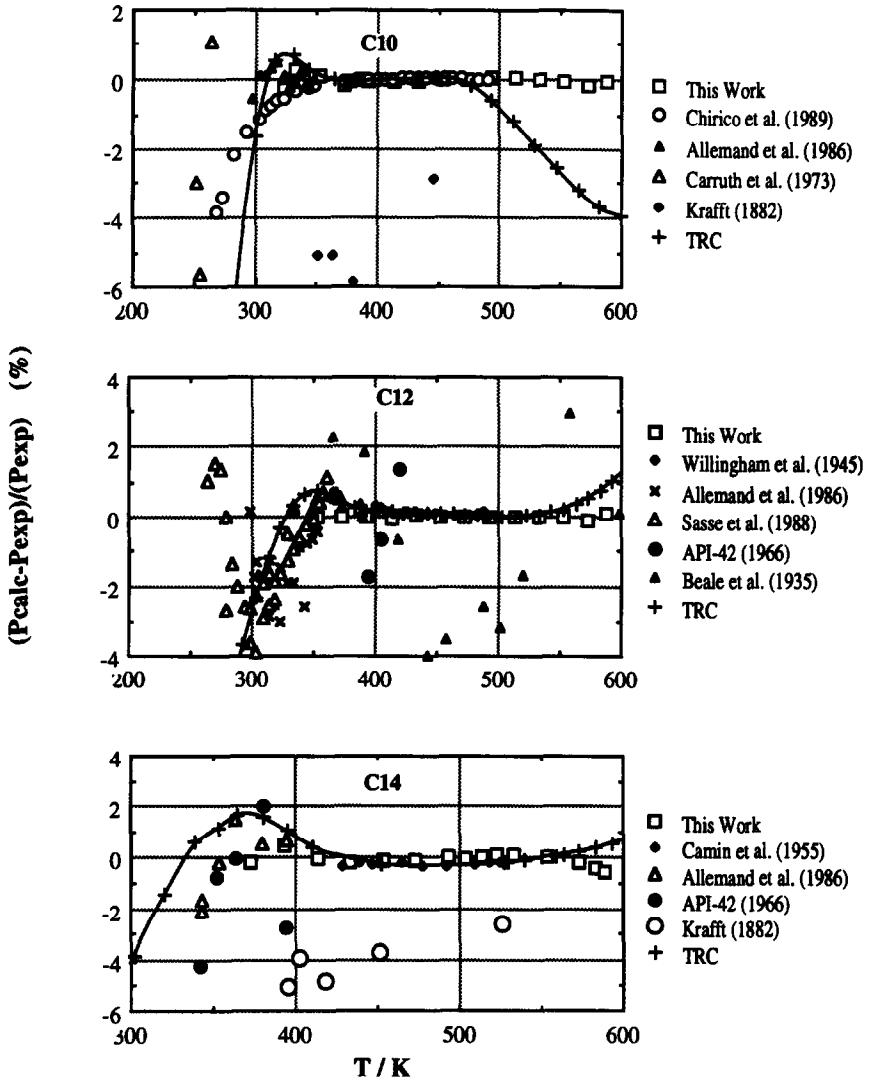

Fig. 6. Deviation plots comparing C_{10}, C_{12}, and C_{14} direct fits in Table 4 with literature vapor pressures.

agreement. Finally, the measurements of Beale and Docksey (1935) for C_{12} are of much lower accuracy and precision than our results.

TRC's extended Antoine correlation for C_{10} rapidly departs from our measurements at temperatures above 500 K. At 600 K, it is 4% higher than our results.

4.3.3. Low-pressure range

The low-pressure measurements of C_{10}, C_{20} and C_{28} made by Chirico et al. (1989) at NIPER using an inclined piston dead weight gauge are among the most accurate modern studies. As Fig. 6 shows, our lowest C_{10} points agree with the NIPER results within 0.5%. When our C_{10} direct

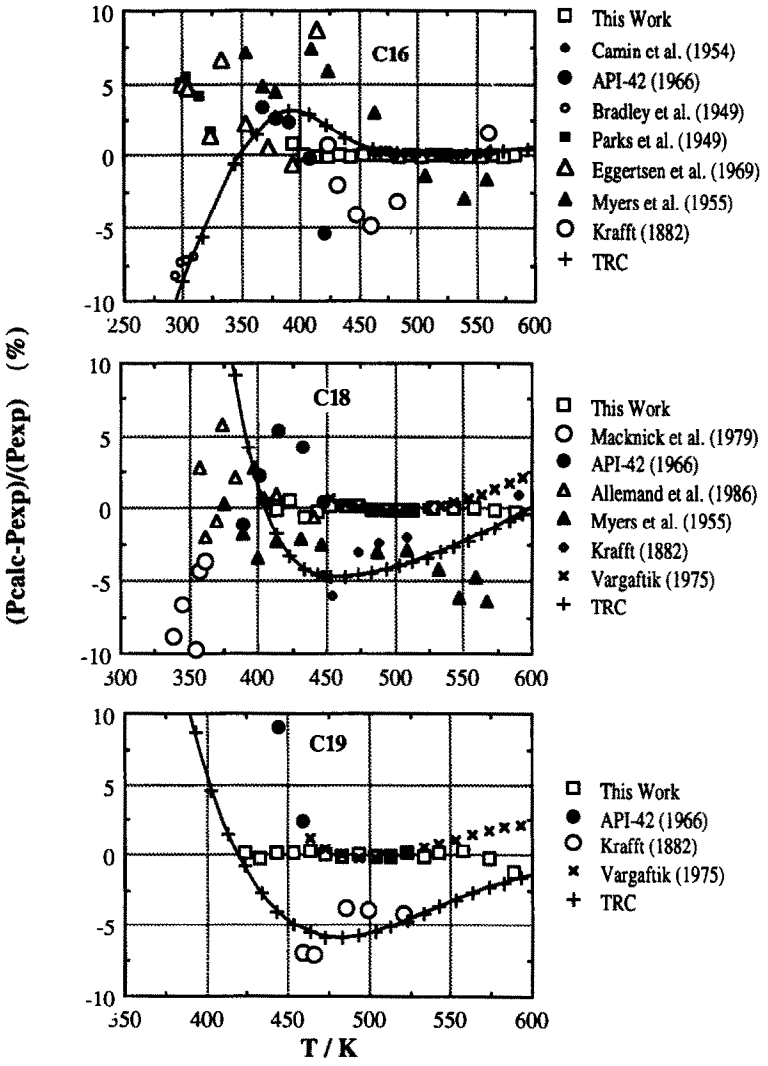

Fig. 7. Deviation plots comparing C_{16}, C_{18} and C_{19} direct fits in Table 4 with literature vapor pressures.

fit is extrapolated 55 K to the lowest temperature of NIPER's C_{10} study, a deviation of only −4% occurs. In contrast, our direct fits for C_{20} and C_{28} in Figs. 8 and 9 appear to degrade much more rapidly when extrapolated to lower temperatures. Our low-pressure data for these two compounds range from 0 to 2.5% higher than the NIPER data.

The direct measurements of Sasse et al. (1988) for C_{12}, C_{20}, C_{22} and C_{24} are of fairly high precision. Direct fits of our data in Table 4 usually agree with their results within 5%. It is unfortunate that the authors studied samples which had relativley low purities (see Table 5).

The gas saturation data of Allemand et al. (1986) for C_{10}, C_{12}, C_{14} and C_{18} coincide with our results. When our C_{12} and C_{14} direct fits are extrapolated downward by 50 K and 30 K, respectively, agreement with the Allemand et al. data is usually within 3% and 2%. As Fig. 6

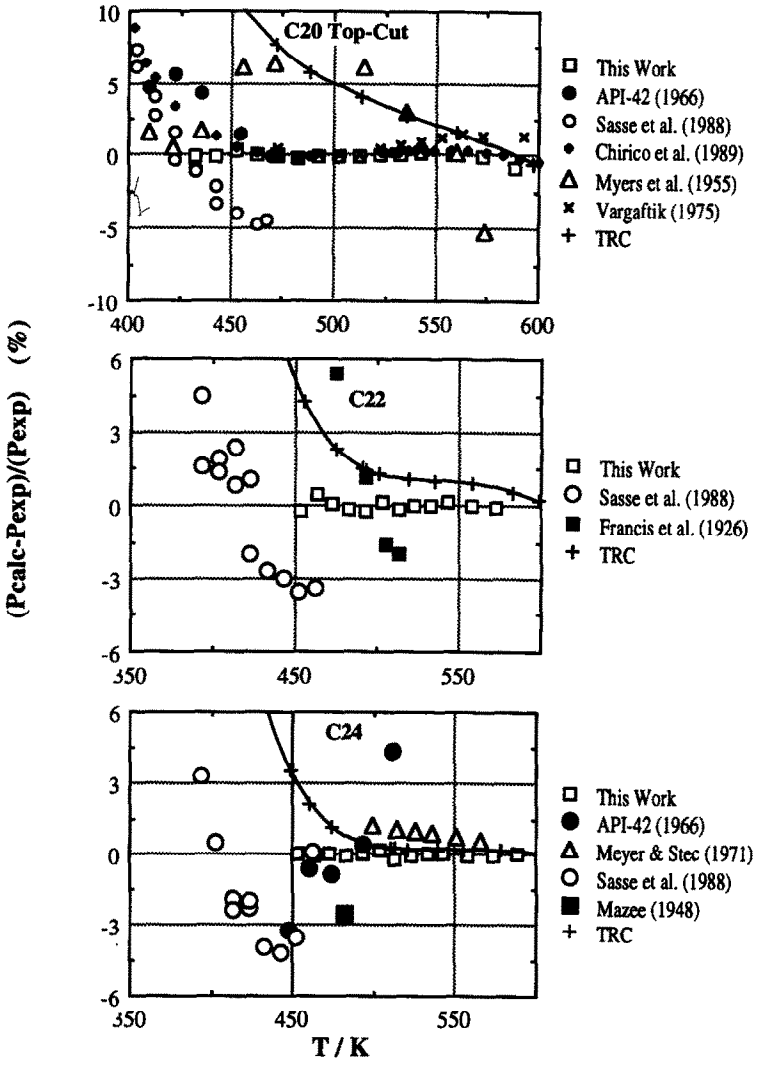

Fig. 8. Deviation plots comparing C_{20}, C_{22} and C_{24} direct fits in Table 4 with literature vapor pressures.

shows, the C_{10} measurements of Allemand et al. fall within 0.3% of our C_{10} direct fit. We have incorporated their C_{10} results into a "conformal" fit, which is presented in Table 6 of the next section. (Note: an even more accurate C_{10} fit, which includes the results of Chirico et al. (1989), is given by Eq. 8.1 in Morgan (1990). The NIPER data became available too late for use in our correlaiton work.)

The C_{18} and C_{20} gas saturation data of Macknick and Prausnitz (1979) were obtained at temperatures as much as 95 K below our measurements. We have incorporated their results into the "conformal" reference equation fits which are discussed in the next section. Direct fits of our vapor pressures for these compounds extrapolate inaccurately into the Macknick and Prausnitz data.

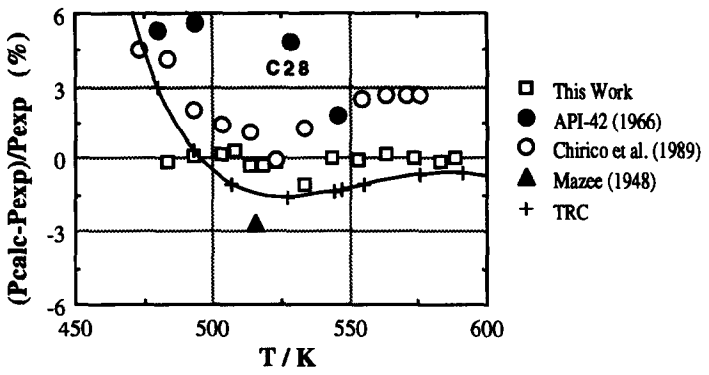

Fig. 9. Deviation plots comparing C_{28} direct fit in Table 4 with literature vapor pressures.

The API Research Project 42, API-42 (1966), presented a table of hydrocarbon boiling points which range between 0.067 and 1.33 kPa. The reported data, which were measured using the methods described by Schiessler and Whitmore (1955), are smoothed. These results agree with our fits and data within 2–5%. The largest discrepancy found is with C_{19}, which averages about 18% higher than our results. We have not depicted all of the C_{19} deviations in Fig. 7.

The effusion measurements of Bradley and Shellard (1949), Parks and Moore (1949), and Morecroft (1964) for compounds in the C_{16}–C_{19} range exhibit considerable scatter. The contradictory nature of this kind of data is best illustrated in Fig. 6 for C_{16}. The Parks and Moore results averge 4% lower than our direct Wagner equation fit while the Bradley and Shellard results average 7% higher. Since our direct fit extrapolates between these two sets of data, it offers a good compromise.

4.3.4. *"Conformal" fits of* n-*alkane vapor pressures*

While some of the direct vapor pressure fits given in Table 4 show good agreement with accurately known data at temperatures below the range of our measurements, other fits extrapolate poorly. We refer to the fits which give an accurate representation of the coexistence range from the critical point down towards the triple point as "conformal" fits. To construct conformal fits for all of the *n*-alkanes of Table 4, we have applied a two-real-fluid CSP method similar to the method applied by Ambrose and Patel (1984). Conformal fits that were constructed out of limited vapor pressure data and use of the two real-fluid CSP method are referred to here as "indirect" fits to distinguish them from our direct fits.

The extrapolation form used by Ambrose and Patel is given in Eq. (9):

$$\ln (P^s/P_c) = \ln P_r^{(R1)} + (\ln P_r^{(R2)} - \ln P_r^{(R1)}) \frac{\omega - \omega_{R1}}{\omega_{R2} - \omega_{R1}} \tag{9}$$

where R1 and R2 are sub- and superscripts which identify the two non-spherical (real) reference fluids, $\ln P_r$ is a reduced vapor pressure reference fluid which is represented by Eq. (6), and ω, the acentric factor, is defined according to Pitzer et al. (1955) in terms of a reduced vapor pressure point at a reduced temperature of $T_r = 0.7$:

$$\omega = -\log_{10} P_r|_{T_r = .7} - 1 \tag{10}$$

Variations of the Ambrose and Patel method include our use of *n*-alkane reference fluids, our use of intermediate sets of parameters, (T_c', P_c', ω') or (T_c'', P_c'', ω''), which have been fitted from vapor pressure to replace temporarily Eq. (9) parameters (T_c, P_c, ω), and our use of a ratio notation "C_{R1}/C_{R2}", where R1 and R2 identify the carbon numbers of the two *n*-alkane reference fluids used in Eq. (9). For consistency, we assume that all of our CSP reference fluids are reduced in terms of the T_c and P_c correlations of Twu (1984), when carbon numbers exceed 9.

For *n*-alkanes, the size of the acentric factor grows roughly in proportion to the carbon number. If the two reference fluids of Eq. (9) have acentric factors, ω_{R1} and ω_{R2}, of similar size as to the test fluid's acentric factor, ω, the use of intermediate parameters is not necessary. In this case, ω can be calculated from the C_{R1}/C_{R2} correlation and use of an accurately known test fluid vapor pressure point. If ω_{R1} and ω_{R2} are much smaller or larger than ω, such as in the case of using the C_1/C_8 correlation to represent the C_{20} coexistence curve, then use of intermediate parameters becomes necessary to force the reference fluids to assume the shape of the test fluid. We have fitted three intermediate parameters (T_c'', P_c'',ω''), from C_{20} vapor pressures which allow C_1/C_8 to represent accurately the C_{20} coexistence curve for $T_r < 0.81$. The intermediate parameters differ from (T_c, P_c, ω) by "shape factors". The use of shape factors for predicting thermodynamic properties has been discussed in a review of the CSP by Leland and Chappelear (1968).

We have employed three kinds of "indirect" fits to extrapolate and smooth limited vapor pressures.

(1) *Indirect-1 fits*: ω is calculated from a single accurate vapor pressure point using known T_c and P_c parameters, and a specified C_{R1}/C_{R2} correlation. The size of reference acentric factors, ω_{R1} and ω_{R2}, should be similar to ω.

(2) *Indirect-2 fits*: T_c is known and parameters P_c' and ω' are fitted from vapor pressures to force C_{R1}/C_{R2} to conform with the data. If the size of ω_{R1} and ω_{R2} are similar to ω, parameters P_c' and ω' will be similar to P_c and ω; otherwise P_c' and ω' will differ from P_c and ω by shape factors.

(3) *Indirect-3 fits*: parameters T_c'', P_c'' and ω'' are fitted from vapor pressure data to force C_{R1}/C_{R2} to conform with the data. Again, this is an application of shape factors.

Results of our efforts to construct conformal fits are summarized in Table 6. The footnotes to the Table describe the data sources, the reference equations and methods employed to determine each fit. Direct fits of data for C_1–C_{16} used weighting functions while the indirect fits for C_{18}, C_{19}, C_{20}, C_{22} and C_{28} were determined by use of the two-real fluid CSP methods, Eq. (9) Asterisks (*) indicate which of the conformal fits in Table 6 differ from direct fits in Table 4. To facilitate comparisons between the fits of Tables 4 and 6, only the vapor pressures of this work have been included in the standard deviation calculations for the C_{10}–C_{28} range.

Further details concerning the conformal fits are given in Morgan and Kobayashi (1994). Deviation plots which compare the conformal fits for the *n*-alkanes, C_{10}–C_{28}, with selected literature correlations and data over the coexistence range are depicted in Figs 5.14–5.23 of Morgan (1990). The temperature scale of these plots is expressed in terms of reduced temperature to emphasize the corresponding states nature of the fits.

Table 6
"Conformal" fits[a] of *n*-alkane vapor pressure data from various sources

Carbon number, *n*	Critical parameters [b]		Acentric factor [c], ω	Wagner equation coefficients [a]				Fit std. dev. [d]	
	T_c (K)	P_c (kPa)		c_1	c_2	c_3	c_4	(%)	Ref.
1	190.551	4599.2	0.0113	−6.0238	1.2706	−0.5748	−1.3717	0.01 D	e
2	305.33	4871.4	0.0990	−6.5094	1.5102	−1.2669	−1.7476	0.06 D	f
3	369.85	4247.5	0.1517	−6.8262	1.7530	−1.8668	−1.8628	0.07 D	g
4	425.16	3796.0	0.1999	−7.0843	1.8199	−2.0795	−2.1481	0.17 D	h
5	469.69	3363.8	0.2507	−7.2659	1.6620	−2.0634	−3.0889	0.02 D	i
6	507.50	3026.8	0.3010	−7.7921	2.5034	−3.3552	−2.1814	0.01 D	j
7	540.10	2734.0	0.3500	−7.9008	2.1890	−3.1966	−3.1973	0.01 D	j,k
8	568.83	2487.0	0.3976	−8.0444	1.9975	−3.1989	−4.0594	3.26 D	j,l
9	594.56	2287.9	0.4450	−8.3087	2.1295	−3.5634	−4.3782	0.05 D	j
* 10	618.86	2119.6	0.4823	−8.4465	2.1216	−3.9030	−4.7213	0.14 D	n
12	659.48	1823.2	0.5642	−8.6543	1.7061	−3.8448	−6.4870	0.05 D	m
14	693.55	1590.0	0.6455	−8.8670	1.3454	−3.9625	−7.3495	0.28 D	m
16	722.59	1404.3	0.7219	−9.3718	1.9330	−5.3984	−6.3172	0.20 D	m
* 18	747.68	1252.8	0.7991	−9.3597	0.9793	−4.7397	−7.9280	0.41 I2	m,p
* 19	759.01	1187.5	0.8379	−9.4540	0.7307	−4.5296	−9.4578	2.40 I1	m,q
* 20	769.63	1128.0	0.8767	−9.5484	0.4821	−4.3194	−10.9881	0.60 I3	r
* 22	789.02	1023.8	0.9498	−9.7526	0.1781	−4.3965	−12.1499	0.39 I1	m,s
24	806.31	935.7	1.0236	−11.2450	3.5501	−9.1470	−8.5039	0.10 D	m
* 28	835.88	795.9	1.1634	−12.0335	4.1113	−10.7606	−9.1177	0.87 I1	m,t

* Conformal fit differs from the direct fit given in Table 4.
[a] Wagner vapor pressure equation, Eq. (6).
[b] T_c and P_c are experimental for $n \leq 9$ and defined by Twu (1984) for $n > 9$.
[c] Vapor pressure from fit is used in Eq. (10).
[d] The fit's percentage standard deviation is defined by Eq. (7). Fit methods: D = direct – used weighting functions; I1 = Indirect-1 – used a pair of *n*-alkane reference fluids, C_{R1}/C_{R2}, and ω calculated from a vapor pressure point to smooth data; I2 = Indirect-2 – data smoothed by fiitting parameters ω' and P_c' for C_{R1}/C_{R2}; I3 = Indirect-3 – data smoothed by fitting parameters T_c'', ω'' and P_c'' for C_{R1}/C_{R2}.
[e] Kleinrahm and Wagner (1986).
[f] Goodwin et al. (1976).
[g] Goodwin and Haynes (1982).
[h] Haynes and Goodwin (1982).
[i] Kratzke et al. (1985) fit.
[j] Willingham et al. (1945).
[k] Forziati et al. (1949) and Smith (1940).
[m] Morgan (1990).
[l] Connolly and Kandalic (1962), Young (1990) and Carruth and Kobayashi (1973).
[p] C_1/C_8 parameters, $P_c' = 1.3238$ MPa and $\omega' = 0.8233$, used in C_2/C_8 to smooth data. Consistent with low-pressure data of Allemand et al. (1986) and Macknick and Prausnitz (1979).
[q] ω calculated from 523 K C_{19} vapor pressure in C_{18}/C_{20}.
[r] Used top-cut C_{20} data of Morgan (1990), API-42 (1966) and Macknick and Prausnitz (1979) to determine $T_c'' = 710$ K, $P_c'' = 0.5482$ MPa, and $\omega'' = 1.15119$ for C_1/C_8.
[s] ω from 543 K C_{22} vapor pressure in C_{10}/C_{20}.
[t] ω from 573 K C_{28} vapor pressure in C_{12}/C_{24}.

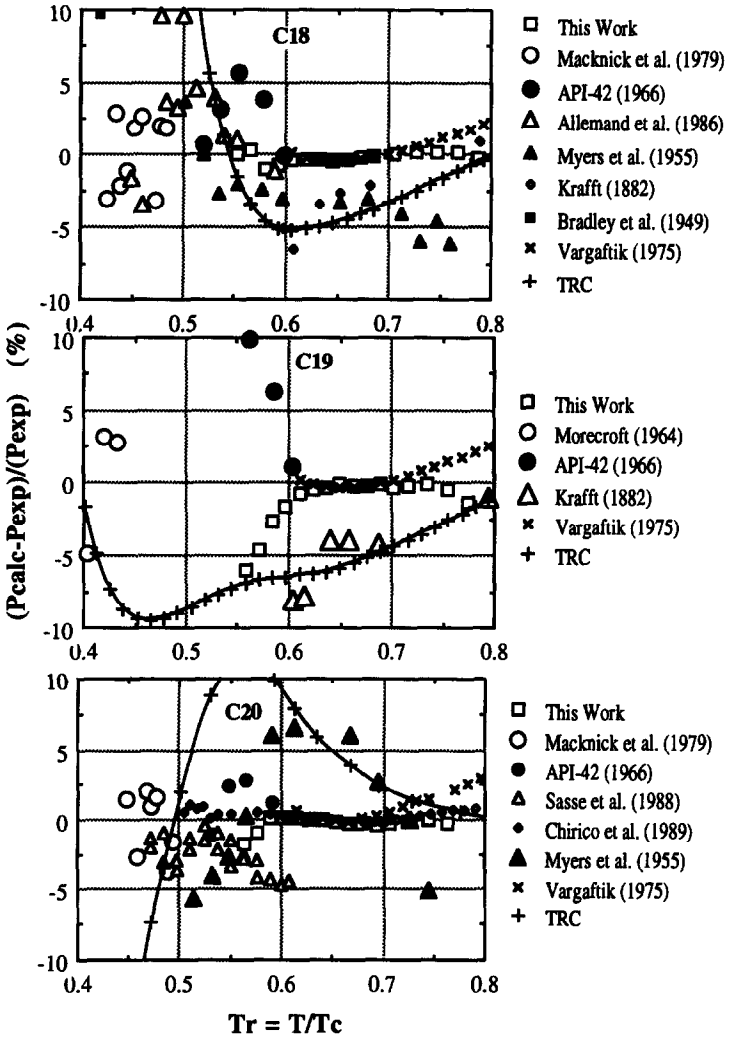

Fig. 10. Deviation plots comparing C_{18}, C_{19} and C_{20} conformal fits in Table 6 with literature vapor pressures; the C_{19} fit is based on the fits for C_{18} and C_{20}.

In Fig. 10, we illustrate an application of the two-real fluid CSP method. Three deviation plots based on the conformal fits of C_{18}, C_{19} and C_{20} are depicted on a reduced temperature scale. As the footnotes to Table 6 indicate, the conformal fit for C_{19} was constructed by applying the C_{18}/C_{20} correlation and a single C_{19} vapor pressure at 523 K which as taken from this work. The C_{19} deviation plot suggests that our low-temperature C_{19} data were adversely affected by the presence of impurities. This explanation is consistent with difficulties experienced while degassing the sample and with freezing curve analyses of the zone-refined C_{19} samples. The C_{18}/C_{20} correlation's excellent prediction of Morecroft's low-pressure effusion data (within 5%) is further testimony to the two real-fluid method. In contrast, the direct fit of C_{19} data in Table 4 (see Fig. 7) extrapolates to Morecroft's data with an average deviation of about 187%.

5. Conclusions

We have presented new static vapor pressure measurements for ten *n*-alkanes in the C_{10}–C_{28} range and given detailed error analyses. The data have been fitted to a "2.5–5" Wagner equation form and compared with selected literature results. We have applied the two-real fluid Corresponding States Principle (CSP) method of Ambrose and Patel (1984) to help extrapolate and smooth data, and to extend the temperature range of some Wagner equation fits. The new results have been used by Morgan (1990) and Morgan and Kobayashi (1994) to extend Pitzer et al. (1955) type CSP correlations to long-chain hydrocarbons.

6. Acknowledgments

Generous financial contributions from the US Department of Energy on Research Contract DE-FG-22-85PC80534 and The Gas Research Institute on Research Contract GRI-5083-260-0963. The Electrical Power Research Institute for usage of equipment. Mr. Raymond Martin for helping to maintain the experimental apparatuses. We also wish to thank AnnaMaria Morgan for her patience and financial sacrifices made while this manuscript was prepared.

References

Allemand, N., Jose, J. and Merlin, J.C., 1986. Mesure des pressions de vapeur d'hydrocarbures C_{10} a C_{18} *n*-alcanes et *n*-alkylbenzenes dans le domaine 3–1000 pascal. Thermochim. Acta, 105: 79–90.

Ambrose, D., 1975. Vapor-pressures. In: Le Neindre, D. and Vodar, B., (eds.), Experimental Thermodynamics, Vol. II. Experimental Thermodynamics of Non-reacting Fluids. Butterworths, London, IUPAC, Chapter 13.

Ambrose, D., 1986. The correlation and estimation of vapour pressures V. Observations on Wagner's method of fitting equations to vapor pressures. J. Chem. Thermodyn., 18: 45–51.

Ambrose, D. and Patel, N.C., 1984. The correlation and estimation of vapor pressures IV. Extrapolation of vapour pressures and estimation of critical pressures by the principle of corresponding states using two reference fluids with nonspherical molecules. J. Chem. Thermodyn., 16: 459–68.

API., 1964. Bibliography of Vapor Pressure Data for Hydrocarbons, Bibliography No. 2. American Petroleum Institute, Division of Refining, Pittsburgh, PA.

API.-42, 1966. Properties of Hydrocarbons of High Molecular Weight Synthesized by Research Project 42 of the American Petroleum Institute. The Pennsylvania State University, University Park, PA.

Beale, E.S.L. and Docksey, P., 1935. A wide range boiling-point conversion chart for hydrocarbons and petroleum products. J. Inst. Pet. Technol., 21: 860–70.

Benedict, R.P., 1984. Fundamentals of Temperature, Pressure and Flow Measurements, 3rd edn. Wiley, New York.

Boublik, T., Fried, V. and Hala, E., 1984. The Vapor Pressures of Pure Substances, 2nd edn. Elsevier, New York.

Bradley, R.S. and Shellard, A.D., 1949. The rate of evaporation of droplets. III. Vapour pressures and rates of evaporation of straight-chain paraffin hydrocarbons. Proc. R. Soc. London, Ser. A, 198: 239–251.

Camin, D.L. and Rossini, F.D., 1955. Physical properties of 14 American Petroleum Institute research hydrocarbons, C_9 to C_{15}. J. Phys. Chem., 59: 1173–79.

Camin, D.L., Forziati, A.F. and Rossini, R.D., 1954. Physical properties of *n*-hexadecane, *n*-decylcyclopentane, *n*-decylcyclohexane, 1-hexadecene and *n*-decylbenzene. J. Phys. Chem., 58: 440–442.

Carruth, G.F. and Kobayashi, R., 1973. Vapor pressures of normal paraffins ethane through *n*-decane from their triple points to about 10 mmHg. J. Chem. Eng. Data, 18(2): 115–126.

Chirico, R.D. Nguyen, A., Steele, W.V., Strube, M.M. and Tsonopoulos, C., 1989. Vapor pressure of *n*-alkanes revisited. New high-precision vapor pressure data on *n*-decane, *n*-eicosane, and *n*-octacosane. J. Chem. Eng. Data, 34: 149–156.

Comité International des Poids et Mesures, 1969. The International Practical Temperature Scale of 1968. Metrologia, 5: 35–44.

Connolly, J.J. and Kandalic, G.A., 1962. Saturation properties and liquid compressibilities for benzene and *n*-octane. J. Chem. Eng. Data, 7: 137–139.

Danner, R.P. and Daubert, T.E. (Eds.), 1983. Technical Data Book – Petroleum Refining, 4th edn. (looseleaf). Refining Dept., American Petroleum Institute, Washington, DC.

Douslin, D.R. and Osborn, A., 1965. Pressure measurements in the 0.01–30 torr range with an inclined-piston gauge. J. Sci. Instrum., 42: 369–73.

Dykyj, J., Repas, M. and Svoboda, J., 1979, 1984. Tlak Nasytenej Pary Organickych Zlucenin. Vydavatelstvo Slovenskej Akademie Vied, Bratislava, Czechoslovakia, Vol. I, 1979; Vol. II, 1984.

Eggertsen. F.T., Sebert, E.E. and Stross, F.H., 1969. Volatility of high organic materials by a flame ionization detection method. Anal. Chem., 41: 1175–79.

Eubank, P.T., Kim, E.S., Holste, J.C. and Hall, K.R., 1987. Effect of impurities upon pure component thermophysical properties. Ind. Eng. Chem. Res., 26: 2020–24.

Forziati, A.F., Norris, W.R. and Rossini, F.D., 1949. Vapor pressures and boiling points of sixty API-NBS hydrocarbons. J. Res. Nat. Bur. Stand., 43: 555–563.

Francis, F. and Wood, N.E., 1926. The boiling points of some higher aliphatic *n*-hydrocarbons. J. Chem. Soc., 129: 1420–23.

Gallagher, J.S. and Morrison, G., 1987. Modelling of impurity effects in fluids and fluid mixtures. J. Chem. Eng. Data, 32: 412–418.

Glasgow, A.R., Jr., Streiff, A.J. and Rossini, F.D., 1945. Determination of the purity of hydrocarbons by measurement of freezing points. J. Res. Nat. Bur. Stand., 35: 355–373.

Goodwin, R.D. and Haynes, W.M., 1982. Thermophysical properties of propane from 85 to 700 K at pressures to 70 MPa. Nat. Bur. Stand. (U.S.) Monogr. 170. US Government Printing Office, Washington DC, 249 pp.

Goodwin, R.D., Roder, H.H. and Straty, G.C., 1976. Thermophysical properties of ethane, from 90 to 600 K at pressures to 700 bar. Nat. Bur. Stand. (U.S.) Tech. Note 684. US Government Printing Office, Washington DC.

Hála, E., Pick, J., Fried, V. and Vilim, O., 1967: Vapour-Liquid Equilibrium, 2nd edn. Pergamon Press, New York.

Haynes, W.M. and Goodwin, R.D., 1982. Thermophysical properties of normal butane from 135 to 700 K at pressures to 70 MPa. Nat. Bur Stand. Monogr. 169. U.S. Government Printing Office, Washington DC, 197 pp.

Herington, E.F.G., 1963. Zone Melting of Organic Compounds. Wiley/Blackwell Scientific, London.

Keistler, J.R. and VanWinkle, M., 1952. Vapor–liquid equilibria at subatmospheric pressures — system dodecane–hexadecane. Ind. Eng. Chem., 44(3): 622–624.

King, M.B. and Mahmud, R.S., 1986. A reduced vapour pressure equation for use at low reduced temperatures. Fluid Phase Equilibria, 27: 309–330.

Kleinrahm, R. and Wagner, W., 1986. Measurement and correlation of the saturated liquid and vapour densities and the vapour pressure along the whole coexistence curve of methane. J. Chem. Thermodynam., 18: 739–760.

Krafft, F., 1882a. Ueber einige höhere Normalparaffine, C_nH_{2n+2}, und ein einfaches Volumgesetz für den tropfbar flüssingen Zustand. I. Chem. Ber., 15: 1687–1712.

Krafft, F., 1882b. Ueber neunzehn höhere Normalparaffine, C_nH_{2n+2}, und ein eingaches Volumgesetz für den tropfbar flüssingen Zustand. II. Chem. Ber., 15: 1711–27.

Krafft, F., 1886. Ueber einige höhere Normalparaffine, C_nH_{2n+2} III. Chem. Ber., 19: 2218–23.

Kratzke, H., Müller, S. Bohn, M. and Kohlen, R., 1985. Thermodynamic properties of saturated and compressed liquid *n*-pentane. J. Chem. Thermodynam., 17: 283–94.

Leland, T.W., Jr. and Chappelear, P.S., 1968. The corresponding states principle. Ind. Eng. Chem., 60: 15–43.

Linder, E.G., 1931. Vapor pressures of some hydrocarbons. J. Phys. Chem, 35(1): 531–35.

Macknick, A.B. and Prausnitz, J.M., 1979. Vapor pressures of high-molecular-weight hydrocarbons. J. Chem. Eng. Data, 24: 175–178.

Mangum, B.W. and Furukawa, G.T., 1990. Guidelines for realizing the international temperature scale of 1990 (ITS-90). NIST Technical Note 1265, Gaithersburg, MD. (176 pages which are distributed to depository libraries in microfiche format.)

Martin, C.B., Martin, R.J., Nasir, P., Wieczorek, S.A., Romanco, W.R., Sivaraman, A., Kragas, T. and Kobayashi, R., 1984. Versatile zone refiner for liquids and low-melting solids. Rev. Sci. Instrum., 55: 1831–33.

Mazee, W.M., 1948. Some properties of hydrocarbons having more than twenty carbon atoms. Recl. Trav. Chim., 67: 197–213.

McGarry, J., 1983. Correlation and prediction of the vapor pressures of pure liquids over large pressure ranges. Ind. Eng. Chem., Process Des. Dev., 22: 313–322.

Meyer, E.F. and Stec, K.S., 1971. Evidence against energetically favored coiling of vapor-phase paraffins up to *n*-tetracosane. J. Am. Chem. Soc., 93: 5451–54.

Morecroft, D.W., 1964. Vapor pressures of some high molecular weight hydrocarbons. J. Chem. Eng. Data, 9: 488–490.

Morgan, D. L., 1990. Extension of Pitzer corresponding states correlations using new vapor pressure measurements of the *n*-alkanes C_{10} to C_{28}. Ph.D. thesis, Rice University. Available through University Microfilms International, 300 N. Zeeb Road, Ann Arbor, MI 48106, USA. Telephone: 313/761-5700 or 800/521-0600.

Morgan, D.L. and Kobayashi, R., 1991. Triple point corresponding states in long-chain *n*-alkanes. Fluid Phase Equilibria, 63: 317–327.

Morgan, D.L. and Kobayashi, R., 1994. Extension of Pitzer CSP models for vapor pressures and heats of vaporization to long-chain hydrocarbons. Fluid Phase Equilibria, 94: 51–87.

Myers, H.S. and Fenske, M.R., 1955. Measurement and correlation of vapor pressure data for high boiling hydrocarbons. Ind. Eng. Chem., 47: 1652–58.

Nasir, P., 1980. Design and development of generalized apparati to study the phase and volumetric behavior of pure components and mixtures at advanced temperatures and pressures, and analytical examination of the resulting observations. Ph.D. thesis, Rice University.

Nasir, P., Hwang, S.C. and Kobayashi, R., 1980. Development of an apparatus to measure vapor pressures at high temperatures and its application to three higher-boiling compounds. J. Chem. Eng. Data, 25: 298–301.

Nesmeyanov, An. N., 1963. Vapor Pressure of the Elements. Academic Press, New York.

O'Hanlon, J.F., 1980. A User's Guide to Vacuum Technology. Wiley, New York.

Ohe, S., 1976. Computer Aided Data Book of Vapor Pressure. Data Book Publishing Co., Tokyo.

Olofsson, G., Angus, S., Armstrong, G.T. and Kormlov, A.N., 1981. A report of IUPAC Commission 1.2 on Thermodynamics. Assignment and presentation of uncertainties of the numerical results of thermodynamic measurements. J. Chem. Thermodyn., 13: 603–622.

Parks, G.S. and Moore, G.E., 1949. Vapor pressure and other thermodynamic data for *n*-hexadecane and *n*-dodecylcyclohexane near room temperature. J. Chem. Phys., 17: 1151–1153.

Partington, J.R., 1951. Advanced Treatise on Physical Chemistry, Vol. 2. Longmans, Green, and Co., New York.

Pfann, W.G., 1958. Zone Melting. Wiley, New York.

Pitzer, K.S., Lippman, D.Z., Curl, R.F., Jr., Huggins, C.M. and Petersen, D.E., 1955. The volumetric and thermodynamic properties of fluids I. Theoretical basis and virial coefficients II. Compressibility factor, vapor pressure and entropy of vaporization. J. Am. Chem. Soc., 77: 3427–40.

Reamer, H.H., Olds, R.H., Sage, B.H. and Lacey, W.N., 1942. Phase equilibria in hydrocarbon systems. Methane–decane system. Ind. Eng. Chem., 34: 1526–31.

Reid, R.C., Prausnitz, J.M. and Poling, B.E., 1987. The Properties of Gases and Liquids, 4th edn. McGraw-Hill, New York.

Roper, V.P., 1988. Derivation of an infinite-dilution activity coefficient model and application to two-component vapor–liquid equilibria data. Ph.D. thesis, Rice University, Houston, TX.

Rosenthal, D.J. and Teja, A.S., 1989. The critical properties of *n*-alkanes using a low-residence time flow apparatus. AIChE J., 35: 1829–1834.

Rossini, F.D., Pitzer, K.S., Arnett, R.L., Braun, R.M. and Pimentel, G.C. (Eds.), 1953. Selected Values of Physical and Thermodynamic Properties of Hydrocarbons and Related Compounds, American Petroleum Institute Research Project 44. Carnegie Press, Pittsburgh, PA.

Ruska, W., Hurt, L.J. and Kobayashi, R., 1970. Circulating pump for high pressure and −200 to +400°C application. Rev. Sci. Instrum., 41: 1444.

Sasse, K., Jose, J. and Merlin, J.-C., 1988. A static apparatus for measurement of low vapor pressures. Experimental results on high molecular-weight hydrocarobons. Fluid Phase Equilibria, 42: 287–304.

Schiessler, R.W. and Whitmore, F.C., 1955. Properties of high molecular weight hydrocarbons. Ind. Eng. Chem., 47: 1660–64.

Scott, D.W. and Osborn, A.G., 1979. Representation of vapor-pressure data. J. Phys. Chem., 83: 2714–23.

Sivaraman, A. and Kobayashi, R., 1982. Investigation of vapor pressures and heats of vaporization of condensed aromatic compounds at elevated temperatures. J. Chem. Eng. Data, 27: 264–269.

Sivaraman, A., Martin, R.J. and Kobayashi, R., 1983. A versatile apparatus to study the vapor pressures and heats of vaporization of carbazole, 9-fluorenone and 9-hydroxyfluorene at elevated temperatures. Fluid Phase Equilibria, 12: 175–188.

Sloan, G.J. and McGhie, A.R., 1988. Techniques of Melt Crystallization. Vol. XIX. In: Weissberger, A. and Saunders, W. (Eds.), Techniques of Chemistry. Wiley, New York.

Smith, E.R., 1940. Boiling points of *n*-heptane and 2,2,4-trimethylpentane over the range 100- to 1,500-millimeter pressures. J. Res. Nat. Bur. Stand., 24: 230–35.

Storvick, T.S. and Park, H.S., 1978. Thermal transpiration: A comparison of experiment and theory. J. Vac. Sci. Technol., 15: 1844–51.

Stull, D.R., 1947. Vapor pressures of pure substances. Ind. Eng. Chem., 39: 517–550.

Tatevskiy, V.M. (Ed.), 1960. Physico-chemical Properties of Individual Hydrocarbons. Gostoptech Press.

Taylor, W.J. and Rossini, F.D., 1944. Theoretical analysis of certain time–temperature freezing and melting curves as applied to hydrocarbons. J. Res. Nat. Bur. Stand., 32: 197–213.

Teja, A.S., 1980. A corresponding states equation for saturated liquid densities, AIChE J. 26: 337–45.

Teja, A.S., Sandler, S.I. and Patel, N.C., 1981. A generalization of the corresponding states principle using two nonspherical reference fluids. Chem. Eng. J., 21: 21–28.

Thodos, G., 1950. Vapor pressures of normal saturated hydrocarbons. Ind. Eng. Chem., 42(5): 1514–26.

TRC, TRC Thermodynamic Tables: Hydrocarbons (formerly API Research Project 44, Selected Values of Hydrocarbons and Related Compounds, see Rossini et al., 1953). Thermodynamics Research Center, The Texas A & M University System, College Station, TX, 77843–3111, USA.

Twu, C.H., 1984. An internally consistent correlation for predicting the critical properties and molecular weights of petroleum and coal-tar liquids. Fluid Phase Equilibria, 16: 137–150.

Vargaftik, N.B., 1975. Handbook of Physical Properties of Liquids and Gases, 2nd edn. (Translation of Spravochnik po Tecplofizicheskim Svoitstvam Gazov i Zhidkostey, published by Nauka Press, Moscow), Hemisphere, Washington, DC.

Ward, S.H. and Van Winkle, M., 1954. Vapor–liquid equilibrium at 200 mm of mercury. Ind. Eng. Chem., 46: 338–350.

Weissberger, A. and Rossiter, B.W. (Eds.), 1971. Techniques of Chemistry, Vol. I. Physical Methods of Chemistry, Part V. Determination of Thermodynamic and Surface Properties. Wiley, New York.

Wieczorek, S.A. and Kobayashi, R., 1980. Vapor pressure measurements of diphenylmethane, thianaphthene, and bicyclohexyl at elevated temperatures. J. Chem. Eng. Data, 25: 302.

Wilcox, W.R., 1964. Zone melting of organic compounds. Chem. Rev., 64: 187–220.

Willingham, C.B., Taylor, W.J., Pignocco, J.M. and Rossini, F.D., 1945. Vapor pressures and boiling points of some paraffin, Alkylcyclopentane, alkylcyclohexane and alkylbenzene hydrocarbons. J. Res. Nat. Bur. Stand., 35: 219–44.

Young, S., 1990. Vapour pressures, specific volumes, and critical constants of normal octane. J. Chem. Soc., 77: 1145–51.

Young, S., 1928. On the boiling points of the normal paraffins at different pressures. Proc. R. Irish Acad., Sect. B, 38: 65–92.

Zwolinski, B.J. and Wilhoit, R.C., 1971. Handbook of Vapor Pressures and Heats of Vaporization of Hydrocarbons and Related Compounds, API44–TRC Publication No. 101. Thermodynamic Research Center, College Station, TX 77843, USA